17. Nakamura H, Lu M, Gwack Y, Souvlis J, Zeichner SL, Jung JU: **Global changes in Kaposi's sarcoma-associated virus gene expression patterns following expression of a tetracycline-inducible Rta transactivator.** *J Virol* 2003, **77**(7):4205–4220.
18. White EA, Clark CL, Sanchez V, Spector DH: **Small internal deletions in the human cytomegalovirus IE2 gene result in nonviable recombinant viruses with differential defects in viral gene expression.** *J Virol* 2004, **78**(4):1817–1830.
19. Pevny LH, Sockanathan S, Placzek M, Lovell-Badge R: **A role for SOX1 in neural determination.** *Development* 1998, **125**(10):1967–1978.
20. Calfon M, Zeng H, Urano F, Till JH, Hubbard SR, Harding HP, Clark SG, Ron D: **IRE1 couples endoplasmic reticulum load to secretory capacity by processing the XBP-1 mRNA.** *Nature* 2002, **415**(6867):92–96.
21. Sidrauski C, Walter P: **The transmembrane kinase Ire1p is a site-specific endonuclease that initiates mRNA splicing in the unfolded protein response.** *Cell* 1997, **90**(6):1031–1039.
22. Scheuner D, Song B, McEwen E, Liu C, Laybutt R, Gillespie P, Saunders T, Bonner-Weir S, Kaufman RJ: **Translational control is required for the unfolded protein response and in vivo glucose homeostasis.** *Mol Cell* 2001, **7**(6):1165–1176.
23. Luo MH, Hannemann H, Kulkarni AS, Schwartz PH, O'Dowd JM, Fortunato EA: **Human cytomegalovirus infection causes premature and abnormal differentiation of human neural progenitor cells.** *J Virol* 2010, **84**(7):3528–3541.
24. Mutnal MB, Cheeran MC, Hu S, Lokensgard JR: **Murine cytomegalovirus infection of neural stem cells alters neurogenesis in the developing brain.** *PLoS One* 2011, **6**(1):e16211.
25. Grassi MP, Clerici F, Perin C, D'Arminio Monforte A, Vago L, Borella M, Boldorini R, Mangoni A: **Microglial nodular encephalitis and ventriculoencephalitis due to cytomegalovirus infection in patients with AIDS: two distinct clinical patterns.** *Clin Infect Dis* 1998, **27**(3):504–508.
26. Perlman JM, Argyle C: **Lethal cytomegalovirus infection in preterm infants: clinical, radiological, and neuropathological findings.** *Ann Neurol* 1992, **31**(1):64–68.
27. Isler JA, Skalet AH, Alwine JC: **Human cytomegalovirus infection activates and regulates the unfolded protein response.** *J Virol* 2005, **79**(11):6890–6899.
28. Skaletskaya A, Bartle LM, Chittenden T, McCormick AL, Mocarski ES, Goldmacher VS: **A cytomegalovirus-encoded inhibitor of apoptosis that suppresses caspase-8 activation.** *Proc Natl Acad Sci U S A* 2001, **98**(14):7829–7834.
29. Terhune S, Torigoi E, Moorman N, Silva M, Qian Z, Shenk T, Yu D: **Human cytomegalovirus UL38 protein blocks apoptosis.** *J Virol* 2007, **81**(7):3109–3123.
30. Schwartz RE, Trehan K, Andrus L, Sheahan TP, Ploss A, Duncan SA, Rice CM, Bhatia SN: **Modeling hepatitis C virus infection using human induced pluripotent stem cells.** *Proc Natl Acad Sci U S A* 2012, **109**(7):2544–2548.
31. Wu X, Robotham JM, Lee E, Dalton S, Kneteman NM, Gilbert DM, Tang H: **Productive hepatitis C virus infection of stem cell-derived hepatocytes reveals a critical transition to viral permissiveness during differentiation.** *PLoS Pathog* 2012, **8**(4):e1002617.
32. Lee KS, Zhou W, Scott-McKean JJ, Emmerling KL, Cai GY, Krah DL, Costa AC, Freed CR, Levin MJ: **Human sensory neurons derived from induced pluripotent stem cells support varicella-zoster virus infection.** *PLoS One* 2012, **7**(12):e53010.
33. D'Aiuto L, Di Maio R, Heath B, Raimondi G, Milosevic J, Watson AM, Bamne M, Parks WT, Yang L, Lin B, *et al*: **Human induced pluripotent stem cell-derived models to investigate human cytomegalovirus infection in neural cells.** *PLoS One* 2012, **7**(11):e49700.

doi:10.1186/2042-4280-4-2
Cite this article as: Nakamura *et al.*: Human cytomegalovirus induces apoptosis in neural stem/progenitor cells derived from induced pluripotent stem cells by generating mitochondrial dysfunction and endoplasmic reticulum stress. *Herpesviridae* 2013 **4**:2.

Biochemical and Biophysical Research Communications 438 (2013) 753–759

Contents lists available at ScienceDirect

Biochemical and Biophysical Research Communications

journal homepage: www.elsevier.com/locate/ybbrc

N-Cadherin is a prospective cell surface marker of human mesenchymal stem cells that have high ability for cardiomyocyte differentiation

Hisako Ishimine [a,b], Norio Yamakawa [a], Mari Sasao [c], Mika Tadokoro [c], Daisuke Kami [d], Shinji Komazaki [e], Makoto Tokuhara [f], Hitomi Takada [a], Yoshimasa Ito [a], Shinichiro Kuno [g], Kotaro Yoshimura [g], Akihiro Umezawa [d], Hajime Ohgushi [c], Makoto Asashima [a,h,i,*], Akira Kurisaki [a,b,*]

[a] Research Center for Stem Cell Engineering, National Institute of Advanced Industrial Science and Technology (AIST), Tsukuba, Ibaraki, Japan
[b] Graduate School of Life and Environmental Sciences, The University of Tsukuba, Tsukuba, Ibaraki, Japan
[c] Health Research Institute, National Institute of Advanced Industrial Science and Technology (AIST), Amagasaki, Hyogo, Japan
[d] Department of Reproductive Biology and Pathology, National Research Institute for Child Health and Development, Setagaya, Tokyo, Japan
[e] Department of Anatomy, Saitama Medical School, Iruma, Saitama, Japan
[f] Department of Surgery, Research Institute National Center for Global Health and Medicine, Shinjuku, Tokyo, Japan
[g] Department of Plastic Surgery, University of Tokyo School of Medicine, Bunkyo, Tokyo, Japan
[h] Department of Life Sciences (Biology), Graduate School of Arts and Sciences, The University of Tokyo, Meguro, Tokyo, Japan
[i] Life Science Center of TARA, The University of Tsukuba, Tsukuba, Ibaraki, Japan

ARTICLE INFO

Article history:
Received 13 July 2013
Available online 27 July 2013

Keywords:
N-cadherin
Flk-1
c-Kit
Cardiomyocyte
Mesenchymal stem cells

ABSTRACT

Mesenchymal stem cells (MSCs) are among the most promising sources of stem cells for regenerative medicine. However, the range of their differentiation ability is very limited. In this study, we explored prospective cell surface markers of human MSCs that readily differentiate into cardiomyocytes. When the cardiomyogenic differentiation potential and the expression of cell surface markers involved in heart development were analyzed using various immortalized human MSC lines, the MSCs with high expression of N-cadherin showed a higher probability of differentiation into beating cardiomyocytes. The differentiated cardiomyocytes expressed terminally differentiated cardiomyocyte-specific markers such as α-actinin, cardiac troponin T, and connexin-43. A similar correlation was observed with primary human MSCs derived from bone marrow and adipose tissue. Moreover, N-cadherin-positive MSCs isolated with N-cadherin antibody-conjugated magnetic beads showed an apparently higher ability to differentiate into cardiomyocytes than the N-cadherin-negative population. Quantitative polymerase chain reaction analyses demonstrated that the N-cadherin-positive population expressed significantly elevated levels of cardiomyogenic progenitor-specific transcription factors, including *Nkx2.5*, *Hand1*, and *GATA4* mRNAs. Our results suggest that N-cadherin is a novel prospective cell surface marker of human MSCs that show a better ability for cardiomyocyte differentiation.

1. Introduction

Stem cell therapy is expected to be an alternative regenerative medicine. In addition to embryonic stem (ES) cells and induced pluripotent stem (iPS) cells, mesenchymal stem cells (MSCs) have been shown to differentiate into various cell types including osteoblasts, chondrocytes, adipocytes, neurons, skeletal muscle fibers, and cardiomyocytes *in vitro*. However, the differentiation ability of MSCs toward cardiomyocytes is still limited [1–3]. To overcome this problem, cell surface markers specific for cardiomyogenic progenitor cells could be used to enrich better population for regenerative medicine of heart failure.

Flk-1, a vascular endothelial growth factor receptor (VEGFR2), has been reported to be a prospective cell surface marker of cardiomyocyte progenitor cells during heart development [4,5]. Flk-1 is expressed in the progenitors of multiple mesodermal lineages, including cardiac, endothelial, and vascular smooth muscle cells [5]. c-Kit (CD117) is a transmembrane tyrosine kinase receptor for Stem cell factor, and used as a cell surface marker for hematopoietic progenitors, melanocytes, mast cells, and spermatogonial stem cells. Recent research has suggested that c-Kit could be a putative cell surface marker for cardiomyogenic progenitor cells in the neonatal heart [6].

A Ca^{2+}-dependent cell–cell adhesion molecule, N-cadherin, is also expressed on cardiomyocyte progenitor cells during mouse development. N-Cadherin expression is observed in the precardiac

* Corresponding authors. Address: Research Center for Stem Cell Engineering, National Institute of Advanced Industrial Science and Technology (AIST), Tsukuba AIST Central 4-1-3105, Higashi 1-1-1, Tsukuba, Ibaraki, 305-8562, Japan. Fax: +81 29 861 2987.
E-mail addresses: asashi@bio.c.u-tokyo.ac.jp (M. Asashima), akikuri@hotmail.com (A. Kurisaki).

0006-291X/$ - see front matter © 2013 Elsevier Inc. All rights reserved.
http://dx.doi.org/10.1016/j.bbrc.2013.07.081

mesoderm at E8.5 in mice and continues to be expressed in the whole heart during development. N-Cadherin-knockout mice died by E10 because of defects in the primitive heart. Although myocardial tissue was initially formed in the knockout mouse embryos, the myocytes were subsequently dissociated, and the heart tube failed to develop [7].

In this study, we explored cell surface markers of human MSCs that have a high ability to differentiate into cardiomyocytes. We show that N-cadherin is a prospective cell surface marker of MSCs with high cardiomyogenic potential.

2. Materials and methods

2.1. Cell culture

Human MSC cell lines, UE7T-13, UE6E7T-11, UBE6T-15, UE6E7T-12, UE7T-9, and UE6E7T-2, were obtained from the JCRB Cell Bank (Osaka, Japan). They were immortalized by retrovirus gene transfer of a combination of *bmi-1*, *E6*, *E7*, and/or *hTERT* genes to human bone marrow stromal cells harvested from a 91-year-old woman [8,10]. The EPC-214 cell line was similarly immortalized at the National Research Institute for Child Health and Development (NRICHD), Japan [9]. These cell lines were maintained in DMEM high glucose (Wako) supplemented with 10% fetal calf serum (FCS; Roche). As for the primary MSCs, ANP0425 and 0607NC, were obtained from Dr. Ohgushi (National Institute of Advanced Industrial Science and Technology, Japan). MSC-R36_2 cells, MSC-R36_3 cells, and Yub623 cells were obtained from the RIKEN BRC Cell Bank (Ibaraki, Japan). Primary MSCs derived from adipose tissue (ASCs), including 09-036 (36) cells, 10-008 (8) cells, 05-055 (55) cells, and 05-076 (76) cells, were prepared at the University of Tokyo, School of Medicine Tokyo, Japan. KN-SC (KN) cells, MY-SC (MY) cells, and NN-SC (NN) cells were prepared at the Research Institute National Center for Global Health and Medicine (NCGM), Japan. Other ASCs were purchased from Invitrogen. For the ASCs, all samples except KN-SC were obtained from women aged 22–45 years (KN-SC was derived from a 41-year-old man). All of these primary cells were maintained in MesenPRO RS Basal Medium supplemented with MesenPRO RS Growth Supplement (GIBCO). Cells were maintained in a humidified incubator at 37 °C with an atmosphere of 5% CO_2. All the experiments using human materials were approved by the Human Ethics Committee at AIST, NRICHD, NCGM, and the University of Tokyo. Human umbilical vein endothelial cells (HUVEC) were cultured in RPMI-1640 supplemented with EGM-2 SingleQuots (LONZA) and penicillin/streptomycin (Wako). TF-1 cells were cultured in RPMI-1640 supplemented with 10% FBS, 2 ng/mL rhGM-CSF, and penicillin/streptomycin (Wako).

2.2. Preparation of mouse fetal cardiomyocytes

The fetal hearts of E16.5 ICR mice were cut into small pieces and washed with phosphate-buffered saline (PBS). They were incubated with 0.15% trypsin and 0.012% EDTA in PBS at 37 °C for 10 min under gentle stirring. The supernatant containing the dissociated cardiomyocytes was mixed with DMEM supplemented with 10% FCS, and centrifuged at 1000 rpm for 5 min. The pellet was then re-suspended in 10 mL of DMEM with 10% FCS and incubated on a glass dish for 1 h to remove fibroblasts. The floating cardiomyocytes were collected and re-plated at $5 \times 10^5/cm^2$ on gelatin-coated glass bottom dishes (Asahi Techno Glass). All the experiments using animals were approved by the Animal Experiment Committee at AIST.

2.3. Immunoblotting analysis

Human MSC cell lines were homogenized in a lysis buffer containing 20 mM Tris–HCl (pH 7.4), 300 mM NaCl, 0.5 mM EDTA, 1% NP-40, and a complete protease inhibitor cocktail (Roche). After centrifugation at 13,000 rpm for 10 min at 4 °C, equal protein amounts were separated by SDS–PAGE (5–20%). The blots were incubated with antibodies against N-cadherin (1:200; C3865, Sigma), Flk-1 (1:100, 10347; IBL), c-Kit (1:200, AF332; R&D Systems), Integrin-α4 (1:200; sc-14008, Santa Cruz), VCAM-1 (1:200; sc-8304, Santa Cruz), PDGFRα (1:200; 323503, BioLegend), Nkx2.5 (1:200; sc-14033, Santa Cruz), GATA4 (1:200; sc-9053, Santa Cruz), or β-tubulin (1:1000, RB-9249; NeoMarkers). Proteins were detected with an enhanced chemiluminescence (ECL) reagent (Super-Signal West Femto Maximum Sensitivity Substrate, Pierce) using an LAS-3000 Image Analyzer (Fuji Film).

2.4. Flow cytometry analysis

All MSCs were harvested with cell dissociation buffer (GIBCO) and blocked with normal sheep IgG on ice for 1 h. Cells were incubated with biotinylated anti-N-cadherin antibody (1:100, BAF1388; R&D System), anti-Flk-1 antibody (1:100, 10347; IBL), and APC-conjugated anti-c-Kit antibody (1:100, 550412; Becton Dickinson) on ice for 1 h. The N-cadherin antibody was fluorescently labeled using Allophycocyanin-Alexa Fluor 750 streptavidin (Molecular Probes). The Flk-1 antibody was fluorescently labeled with the Alexa Fluor 488-conjugated secondary antibody (Molecular Probes). Cells were resuspended in buffer with propidium iodide (Sigma). Analysis was performed with a FACS Aria (Becton Dickinson) and FlowJo software (TOMY Digital Biology) with propidium iodide-negative population. The data were obtained from at least two independent experiments.

3. Results

MSCs are a mixture of primary adherent cells derived from the stroma of adult tissues. The multipotency of MSCs rapidly decreases as the passage number increases. Therefore, it is not easy to obtain reproducible data from these heterogeneous primary cells. To overcome these problems, we took advantage of immortalized human MSC clones with *bmi-1*, *TERT*, *E6*, and/or *E7*, which retain their multipotent differentiation ability over a long time when cultured *in vitro* [8].

Cardiac differentiation of human MSCs was performed by co-culturing with mouse fetal cardiomyocytes, which is a well-established method to differentiate MSCs into electro-physiologically validated cardiomyocytes [9,10]. Human MSC cell lines were labeled with a GFP-expressing lentivirus and then cultured on a cardiomyocyte feeder cells prepared from mouse embryonic heart tissue (Fig. S1A). On day 7, human MSC lines such as EPC-214 and UE7T-13 differentiated into cardiomyocytes. Around 5% of these GFP-labeled MSCs differentiated into beating cardiomyocytes (Fig. 1A). GFP-positive, differentiated cardiomyocytes showed autonomously periodical contractions (Fig. S1B). Significant number of GFP-positive human MSCs expressed cardiomyocyte-specific terminal differentiation markers (Fig. S1C, left and middle, Fig. S1D, left, and a confocal image Fig. S1E). On the other hand, some cell lines did not differentiate into beating cardiomyocytes under identical conditions (UE7T-9, UE6E7T-2) (Fig. S1C right and Fig. S1D right).

Next, the efficiency of human MSCs differentiation into spontaneously beating cardiomyocytes was quantified by counting the number of GFP-positive and spontaneously beating cardiomyocytes with a fluorescence microscope on day 7 (Fig. 1A). The

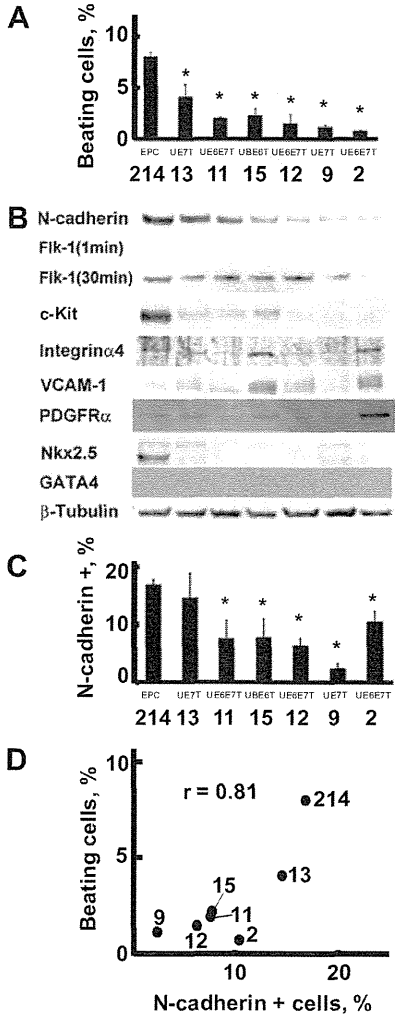

Fig. 1. Correlation between cardiomyogenic differentiation efficiency and cell surface protein marker expression in human MSC cell lines. (A) Autonomously beating cardiomyocytes differentiated from GFP-labeled human MSC lines, EPC-214, UE7T-13, UE6E7T-11, UBE6T-15, UE6E7T-12, UE7T-9, and UE6E7T-2, were counted under a fluorescence microscope. (B) The expression of cell surface proteins and transcription factors related to cardiovascular development were analyzed by immunoblotting of whole cell lysates. (C) Flow cytometric analysis of cell surface expression of N-cadherin in human MSC lines. (D) Correlation between the differentiation efficiency into cardiomyocytes and cell surface N-cadherin expression in human MSC lines. The vertical axis represents the differentiation efficiency. The horizontal axis represents cell surface expression of N-cadherin. The correlation coefficient (r) is shown on the graph. *$P < 0.05$.

expression of various cell surface proteins, which are essential for the development of the heart *in vivo* or are specifically expressed in cardiovascular progenitor cells, was examined by immunoblotting (Fig. 1B). Among these markers, the expression of N-cadherin showed a good correlation with the differentiation efficiency toward beating cardiomyocytes. The MSC lines highly expressing N-cadherin showed higher differentiation ability toward cardiomyocytes. Flk-1 also showed an expression pattern similar to that of N-cadherin. However, the expression levels in human MSCs were very low. Only an extremely long exposure (30 min) enabled us to detect the Flk-1 protein bands (Fig. 1B). The expression of c-Kit showed some correlation with the cardiomyogenic differentiation abilities of these cells, although the expression levels of c-Kit in some human MSCs that readily differentiated into cardiomyocytes were very low (Fig. 1B, UE7T-13, UE6E7T-11, and UBE6T-15).

Other cell surface proteins have been reported as essential for heart development. Integrin α4 is essential for the development of the heart and placenta [11]; a homozygous null mutant of integrin α4 caused embryonic lethality due to defects in the epicardium and coronary vessel development, leading to cardiac hemorrhage, in addition to failure of fusion between the allantois and chorion during placentation. Knockout mice of vascular cell adhesion molecule 1 (VCAM-1) displayed a reduction in the compact layer of the ventricular myocardium and intraventricular septum [12]. Platelet-derived growth factor receptor α (Pdgfrα) is expressed in cardiac progenitor cells in the posterior part of the secondary heart field. Pdgfrα is also expressed in the valves and pericardia of the heart at E12.5–16.5 [13]. However, the expression of these cell surface proteins did not show a strong correlation with the differentiation ability of human MSCs into cardiomyocytes (Fig. 1A and B).

Next, we verified the cell surface-specific expression of N-cadherin, Flk-1, and c-Kit in living MSCs by flow cytometry. Flk-1 was barely detectable on the cell surface of human MSCs (Fig. 2A), although a positive control, HUVEC, showed strong cell surface expression of Flk-1 (Fig. 2A, right), indicating that human MSCs do not express detectable amounts of Flk-1 on the plasma membrane. The cell surface expression of c-Kit was also relatively low (Fig. 2B), and the MSC lines with higher differentiation ability toward cardiomyocytes did not show a significant amount of cell surface expression of c-Kit (Fig. 2B, UE7T-13).

By contrast, N-cadherin was readily detectable in the human MSC lines with high differentiation ability toward beating cardiomyocytes (Fig. 2C). When the cell surface expression of N-cadherin (Fig. 1C) and the differentiation ability into beating cardiomyocytes (Fig. 1A) were compared with human MSC cell lines, a strong correlation was observed between these 2 events ($r = 0.81$; Fig. 1D). Immunofluorescence analysis of the human MSC line EPC-214, which readily differentiated into cardiomyocytes, showed characteristic localization of N-cadherin in cell-to-cell contacts in addition to the uniform expression on the plasma membrane (Fig. 2D). However, UE7T-9 cells, which expressed N-cadherin at low levels and did not differentiate into cardiomyocytes, did not show significant expression of N-cadherin (Fig. 2D, right). These results suggest that N-cadherin could be a good prospective cell surface marker of cardiomyogenic human MSCs.

Next, we validated the expression of N-cadherin with various primary human MSCs. Human bone marrow-derives MSCs (BMSCs) cultured for a limited number of passages gave a good correlation between the cell surface expression of N-cadherin and the differentiation ability into beating cardiomyocytes (Fig. 3A and B). Human MSCs derived from adipose tissue (ASCs) also showed similar results (Fig. 3D and E). The Pearson's correlation coefficients of cell surface expression of N-cadherin and differentiation efficiency toward beating cardiomyocytes in BMSCs and ASCs were good in both cases (0.55 and 0.77, respectively; Fig. 3C and F). As for c-Kit, we failed to detect significant expression of c-Kit in primary MSCs that showed distinct cardiomyogenic differentiation abilities (Fig. S2, 36_2). c-Kit protein could be detected on the cell surface of some primary ASCs (Fig. S2B, 1212). However, the isolation of c-Kit-positive cells from these primary ASCs was not successful by flow cytometry.

To determine whether the N-cadherin-positive population of human MSCs has higher differentiation ability into cardiomyocytes than N-cadherin-negative MSCs, we established the separation conditions of N-cadherin-positive cells using MACS (Fig. S3). Then, the N-cadherin-positive fraction was concentrated from a primary culture of human ASCs (1212 used in Fig. 3) using the same method (Fig. 4A); these cells were further cultured on mouse embryonic heart feeder cells for 7 days. The enriched ASC fraction expressing cell surface N-cadherin showed a 4-fold higher cardiomyogenic differentiation ability than the N-cadherin-negative fraction (Fig. 4B).

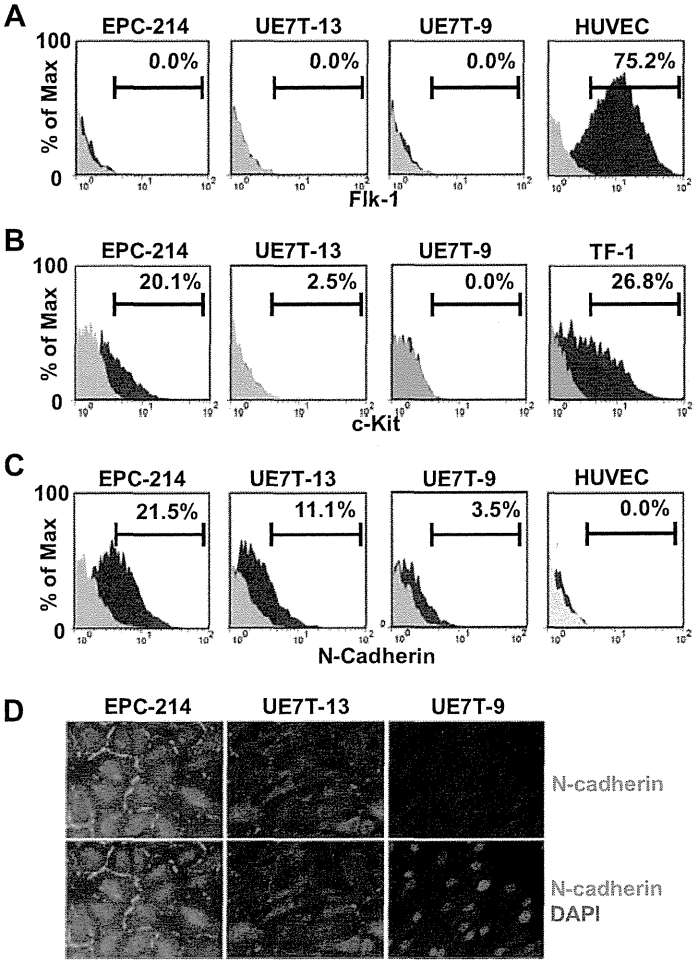

Fig. 2. Representative FACS plots of cell surface protein expression in human MSC cell lines. The live cells were immunostained with (A) Flk-1, (B) c-Kit, or (C) N-cadherin antibodies. Propidium iodide-positive cells were excluded from the analysis. (D) Localization of N-cadherin in human MSCs. The indicated human MSC lines were immunostained with N-cadherin antibody (green) and DAPI (blue). (For interpretation of the references to colour in this figure legend, the reader is referred to the web version of this article.)

To characterize the cardiomyogenic N-cadherin-positive population, we analyzed the gene expression profiles of the MACS-sorted fractions with microarray. Gene ontology analysis of 3056 genes (among 44,000 genes) that exhibited more than a 1.5-fold difference identified molecular functions associated with zinc ion binding, transition metal ion binding, and nucleic acid binding (Fig. S4A) and biological functions involved in DNA binding, gene expression, transcription, and metabolic processes of nucleic acid (Fig. S4B). These results suggested that N-cadherin-positive cells showed higher expression of specific DNA-binding proteins and elevated metabolic activity. On the other hand, the N-cadherin-negative population showed higher expression of genes involved in the MHC class I protein complex, vacuole organization, and GTPase activity (Fig. S4C and S4D).

When the expression of various lineage marker genes was compared, the N-cadherin-positive fraction showed up-regulated expression of genes involved in the differentiation of cardiomyocytes and skeletal myocytes, such as *Nkx2.5*, *Hand1*, *Tnni3* (*cTnI*), and *Myog* (Fig. 4C). In contrast, ectodermal and endodermal lineage markers were the same among the MACS-sorted fractions, with the exception of *Pax4*, a transcription factor involved in pancreatic development. Although MSCs efficiently differentiate into osteoblasts, chondrocytes, and adipocytes, these specific markers did not show a large difference. The expression of MSC-specific cell surface markers was not increased in the N-cadherin-positive fraction.

Quantitative PCR analysis revealed significant up-regulation of a cardiomyogenic precursor-specific gene, *Nkx2.5*, in the N-cadherin-positive fraction, for more than 200-times higher than that in the N-cadherin-negative fraction. Two other transcription factors, *Hand1* and *Gata4*, but not Tbx5, also showed significantly elevated expression in the N-cadherin-positive fraction (Fig. 4D). Interestingly, the expression of *Myog*, a transcription factor involved in skeletal muscle development, was also elevated in the N-cadherin-positive fraction. Although terminal markers for cardiomyocytes, such as *Anp* and *cTnI*, showed higher expression in the N-cadherin-positive fraction (Fig. 4E), the expression levels of these terminal markers were very low, suggesting that N-cadherin-positive cells may be ready for differentiation, but not terminally differentiated into cardiomyocytes.

Interestingly, the expression of some pluripotency-specific genes such as *Oct4* (*Pou5f1*), *Sall4*, and *Nanog* was significantly up-regulated in the N-cadherin-positive population (Fig. 4F and G). However, these expression in human MSCs was not as high as that in human ES cells (Fig. 4F), suggesting that these genes up-regulated in N-cadherin-positive MSCs may not exhibit pluripotency as observed in ES/iPS cells.

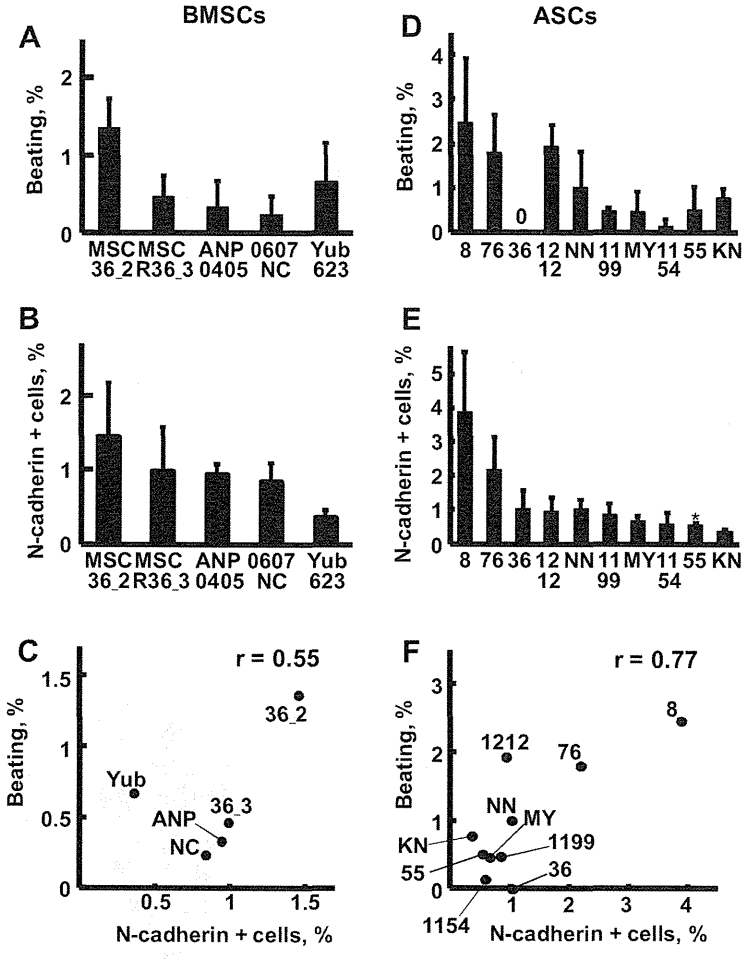

Fig. 3. Differentiation efficiency of primary human MSCs into cardiomyocytes and cell surface expression of N-cadherin. In this experiment, primary human MSCs derived from (A–C) the bone marrow (BMSCs) or (D–F) adipose-derived tissue (ASCs) were used. (A, D) Differentiation efficiency of primary human MSCs into cardiomyocytes. Autonomously beating cardiomyocytes differentiated from GFP-labeled human (A) BMSCs or (D) ASCs were counted using a microscope. (B, E) Flow cytometric analysis of cell surface expression of N-cadherin in primary human (B) BMSCs or (E) ASCs. *$P < 0.05$. (C, F) Correlation between the differentiation efficiency into beating cardiomyocytes and the cell surface N-cadherin expression of primary human (C) BMSCs or (F) ASCs. The correlation coefficient (r) is shown on the graph.

4. Discussion

In this study, we have identified N-cadherin as a reliable cell surface marker for human MSCs with higher differentiation ability toward cardiomyocytes. N-cadherin is continuously expressed from cardiomyogenic progenitor cells to mature cardiomyocytes in the adult heart. N-cadherin maintains the functional gap junction complex at the plasma membrane in the adult heart, and conditional knockout of N-cadherin in mice resulted in arrhythmia in adult hearts with significant decreases in Cn43 and Cn40 [17].

We have previously shown that the cardiomyogenic progenitor cells differentiated from mouse ES cells expressed high levels of N-cadherin on the cell surface membrane, and an antibody against N-cadherin could be used to concentrate the progenitor cells from a heterogeneous cell population differentiated from mouse ES cells [18]. Although the possible differentiation pathway of cardiomyocytes from pluripotent ES cells and multipotent MSCs may not be the same, N-cadherin could be a common progenitor marker of the cardiomyogenic cells derived from these stem cells.

In addition to cardiomyogenic genes, we observed increased expression of pluripotency-specific transcription factors of ES cells, such as *Oct4*, *Sall4*, and *Nanog*, in the N-cadherin-positive fraction. Recently, *Oct4* has been suggested to be the gatekeeper into and out of the reprogramming expressway [19]. Therefore, the elevated expression of *Oct4* and related transcription factors could positively modulate the differentiation ability of MSCs. For example, overexpression of the *Oct4* gene enhanced the differentiation ability of MSCs [14], and knockdown of *Oct4* caused loss of multiple differentiation potential [15]. Nanog was also shown to possess similar activity in BMSCs [16]. Therefore, N-cadherin-positive cells with up-regulated expression of *Oct4* and other transcription factors responsible for cardiomyogenesis may increase the differentiation ability of MSCs into cardiomyocytes.

N-Cadherin is localized in the cell–cell contacts of cardiomyocytes and plays essential roles for formation of the cardiac intercalated disk structure that electromechanically couples adjacent cardiac myocytes. Addition of antibodies against N-cadherin to the cultured cardiomyocytes [20], mesodermal explants [21] or injected into embryos [22] caused a reduction in the number of myofibrils and destroy stress fibers [23]. In primary cardiomyocytes dissociated from adult rat heart, N-cadherin diffusely distributed around the cell periphery begins to co-localize with desmocollin, plakoglobin, and plakophilin-2 at the cell contact sites. The newly generated adhesive contacts sequentially recruit desmoplakin, intermediate filaments, connexin-43, and ankyrin-G. Subsequently, the voltage-gated sodium channel is incorporated into mature intercalated disks. This assembly process requires the clustering of transmembrane adhesive contacts with N-cadherin

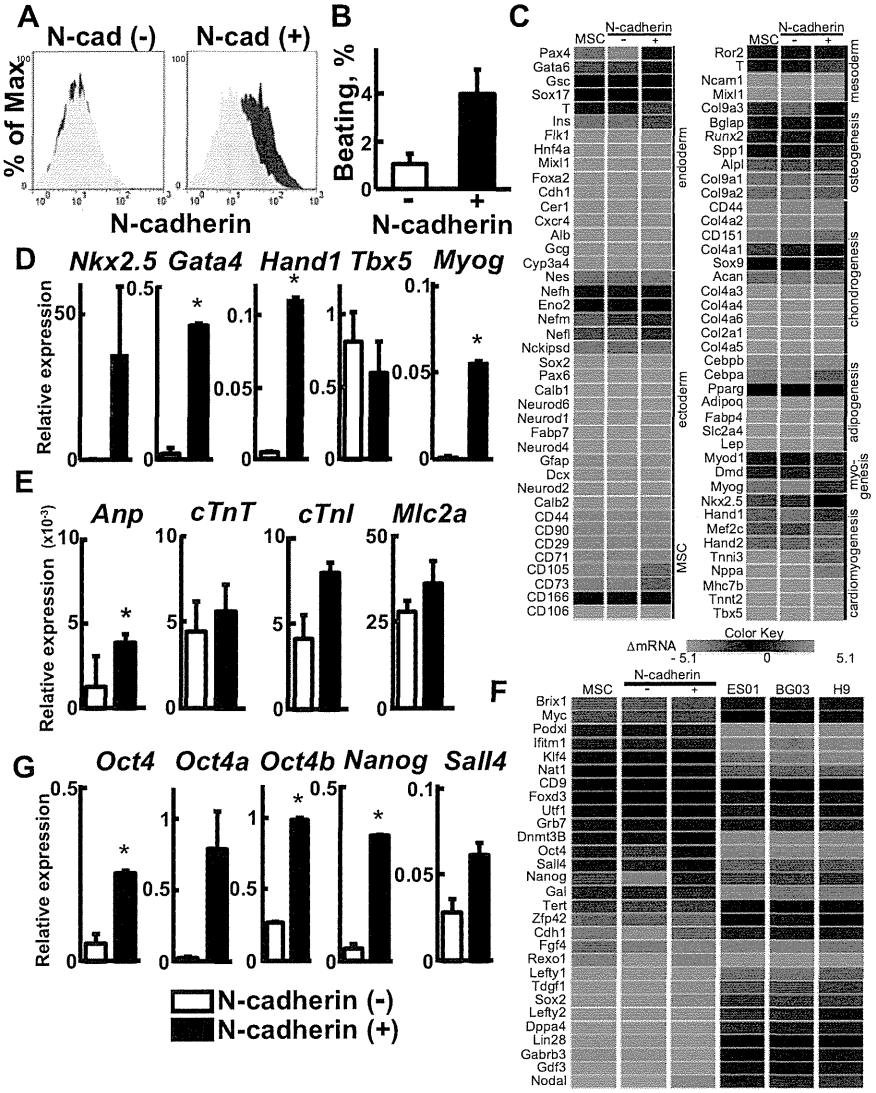

Fig. 4. Separation of N-cadherin-positive cells from the primary MSCs derived from adipose tissue (1212) with anti-N-cadherin antibody-conjugated magnetic beads. (A) The FACS histograms represent cell surface N-cadherin expression in the N-cadherin-negative fraction (left) and N-cadherin-positive fraction (right). (B) Differentiation efficiency of the purified primary ASCs into beating cardiomyocytes. Bar graphs represent the mean value of differentiation efficiency obtained from two independent experiments. (C) Heat map profile of lineage-specific differentiation marker expression in ASCs. The N-cadherin-positive fraction showed elevated expression of specific genes involved in cardiomyogenesis. (D, E) qPCR analysis of cardiomyogenic progenitor-specific transcription factors (D) and terminal differentiation markers for heart development (E). (F) Heat map profile of pluripotency-specific marker expression in human ASCs and human ES cells (ES01, BG03, and H9). (G) qPCR analysis of the expression of pluripotency-specific transcription factors in MACS-sorted fractions. $^{*}P < 0.05$. (For interpretation of the references to colour in (C) and (F), the reader is referred to the web version of this article.)

[24]. Therefore, MSCs with higher expression of N-cadherin may have preferable potential for the differentiation into cardiomyocytes. N-cadherin is expressed in pericytes and is involved in the interaction between pericytes and endothelial cells during vessel formation *in vivo* [25,26]. Pericytes in MSCs could be one of the possible cell sources that show higher differentiation ability toward cardiomyocytes.

Disclosure statement

No competing financial interests exist.

Acknowledgments

We would like to thank to Dr. Yuzuru Ito for discussion. The lentiviral vector for GFP was provided by Dr. Miyoshi (Riken BRC) through the National Bio-Resource Project of the MEXT, Japan. This research was supported by NEDO of Japan (New Energy and Industrial Development Organization, Translational Research Promotion Project).

Appendix A. Supplementary data

Supplementary data associated with this article can be found, in the online version, at http://dx.doi.org/10.1016/j.bbrc.2013.07.081.

References

[1] M. Shiota, T. Heike, M. Haruyama, S. Baba, A. Tsuchiya, H. Fujino, H. Kobayashi, T. Kato, K. Umeda, M. Yoshimoto, T. Nakahata, Isolation and characterization of bone marrow-derived mesenchymal progenitor cells with myogenic and neuronal properties, Exp. Cell Res. 313 (2007) 1008–1023.

[2] S. Wakitani, T. Saito, A.I. Caplan, Myogenic cells derived from rat bone marrow mesenchymal stem cells exposed to 5-azacytidine, Muscle Nerve 18 (1995) 1417–1426.

[3] S. Makino, K. Fukuda, S. Miyoshi, F. Konishi, H. Kodama, J. Pan, M. Sano, T. Takahashi, S. Hori, H. Abe, J. Hata, A. Umezawa, S. Ogawa, Cardiomyocytes can be generated from marrow stromal cells in vitro, J. Clin. Invest. 103 (1999) 697–705.
[4] J.K. Yamashita, M. Takano, M. Hiraoka-Kanie, C. Shimazu, Y. Peishi, K. Yanagi, A. Nakano, E. Inoue, F. Kita, S. Nishikawa, Prospective identification of cardiac progenitors by a novel single cell-based cardiomyocyte induction, FASEB J. 19 (2005) 1534–1536.
[5] S.J. Kattman, T.L. Huber, G.M. Keller, Multipotent flk-1+ cardiovascular progenitor cells give rise to the cardiomyocyte, endothelial, and vascular smooth muscle lineages, Dev. Cell 11 (2006) 723–732.
[6] Y.N. Tallini, K.S. Greene, M. Craven, A. Spealman, M. Breitbach, J. Smith, P.J. Fisher, M. Steffey, M. Hesse, R.M. Doran, A. Woods, B. Singh, A. Yen, B.K. Fleischmann, M.I. Kotlikoff, C-kit expression identifies cardiovascular precursors in the neonatal heart, Proc. Natl. Acad. Sci. USA 106 (2009) 1808–1813.
[7] G.L. Radice, H. Rayburn, H. Matsunami, K.A. Knudsen, M. Takeichi, R.O. Hynes, Developmental defects in mouse embryos lacking N-cadherin, Dev. Biol. 181 (1997) 64–78.
[8] T. Mori, T. Kiyono, H. Imabayashi, Y. Takeda, K. Tsuchiya, S. Miyoshi, H. Makino, K. Matsumoto, H. Saito, S. Ogawa, M. Sakamoto, J. Hata, A. Umezawa, Combination of hTERT and bmi-1, E6, or E7 induces prolongation of the life span of bone marrow stromal cells from an elderly donor without affecting their neurogenic potential, Mol. Cell. Biol. 25 (2005) 5183–5195.
[9] K. Okamoto, S. Miyoshi, M. Toyoda, N. Hida, Y. Ikegami, H. Makino, N. Nishiyama, H. Tsuji, C.H. Cui, K. Segawa, T. Uyama, D. Kami, K. Miyado, H. Asada, K. Matsumoto, H. Saito, Y. Yoshimura, S. Ogawa, R. Aeba, R. Yozu, A. Umezawa, 'Working' cardiomyocytes exhibiting plateau action potentials from human placenta-derived extraembryonic mesodermal cells, Exp. Cell Res. 313 (2007) 2550–2562.
[10] Y. Takeda, T. Mori, H. Imabayashi, T. Kiyono, S. Gojo, S. Miyoshi, N. Hida, M. Ita, K. Segawa, S. Ogawa, M. Sakamoto, S. Nakamura, A. Umezawa, Can the life span of human marrow stromal cells be prolonged by bmi-1, E6, E7, and/or telomerase without affecting cardiomyogenic differentiation?, J Gene Med. 6 (2004) 833–845.
[11] J.T. Yang, H. Rayburn, R.O. Hynes, Cell adhesion events mediated by alpha 4 integrins are essential in placental and cardiac development, Development 121 (1995) 549–560.
[12] L. Kwee, H.S. Baldwin, H.M. Shen, C.L. Stewart, C. Buck, C.A. Buck, M.A. Labow, Defective development of the embryonic and extraembryonic circulatory systems in vascular cell adhesion molecule (VCAM-1) deficient mice, Development 121 (1995) 489–503.
[13] N. Takakura, H. Yoshida, Y. Ogura, H. Kataoka, S. Nishikawa, PDGFR alpha expression during mouse embryogenesis: immunolocalization analyzed by whole-mount immunohistostaining using the monoclonal anti-mouse PDGFR alpha antibody APA5, J. Histochem. Cytochem. 45 (1997) 883–893.
[14] T.M. Liu, Y.N. Wu, X.M. Guo, J.H. Hui, E.H. Lee, B. Lim, Effects of ectopic Nanog and Oct4 overexpression on mesenchymal stem cells, Stem Cells Dev. 18 (2009) 1013–1022.
[15] C.C. Tsai, P.F. Su, Y.F. Huang, T.L. Yew, S.C. Hung, Oct4 and Nanog directly regulate Dnmt1 to maintain self-renewal and undifferentiated state in mesenchymal stem cells, Mol. Cell 47 (2012) 169–182.
[16] M.J. Go, C. Takenaka, H. Ohgushi, Forced expression of Sox2 or Nanog in human bone marrow derived mesenchymal stem cells maintains their expansion and differentiation capabilities, Exp. Cell Res. 314 (2008) 1147–1154.
[17] J. Li, V.V. Patel, I. Kostetskii, Y. Xiong, A.F. Chu, J.T. Jacobson, C. Yu, G.E. Morley, J.D. Molkentin, G.L. Radice, Cardiac-specific loss of N-cadherin leads to alteration in connexins with conduction slowing and arrhythmogenesis, Circ. Res. 97 (2005) 474–481.
[18] M. Honda, A. Kurisaki, K. Ohnuma, H. Okochi, T.S. Hamazaki, M. Asashima, N-cadherin is a useful marker for the progenitor of cardiomyocytes differentiated from mouse ES cells in serum-free condition, Biochem. Biophys. Res. Commun. 351 (2006) 877–882.
[19] J. Sterneckert, S. Hoing, H.R. Scholer, Concise review: Oct4 and more: the reprogramming expressway, Stem Cells 30 (2012) 15–21.
[20] A.P. Soler, K.A. Knudsen, N-cadherin involvement in cardiac myocyte interaction and myofibrillogenesis, Dev. Biol. 162 (1994) 9–17.
[21] K. Imanaka-Yoshida, K.A. Knudsen, K.K. Linask, N-cadherin is required for the differentiation and initial myofibrillogenesis of chick cardiomyocytes, Cell Motil. Cytoskeleton 39 (1998) 52–62.
[22] K.K. Linask, K.A. Knudsen, Y.H. Gui, N-cadherin-catenin interaction: necessary component of cardiac cell compartmentalization during early vertebrate heart development, Dev. Biol. 185 (1997) 148–164.
[23] T. Volk, B. Geiger, A-CAM: a 135-kD receptor of intercellular adherens junctions. I. Immunoelectron microscopic localization and biochemical studies, J. Cell Biol. 103 (1986) 1441–1450.
[24] S.B. Geisler, K.J. Green, L.L. Isom, S. Meshinchi, J.R. Martens, M. Delmar, M.W. Russell, Ordered assembly of the adhesive and electrochemical connections within newly formed intercalated disks in primary cultures of adult rat cardiomyocytes, J. Biomed. Biotechnol. 2010 (2010) 624719.
[25] H. Gerhardt, H. Wolburg, C. Redies, N-cadherin mediates pericytic-endothelial interaction during brain angiogenesis in the chicken, Dev. Dyn. 218 (2000) 472–479.
[26] E. Tillet, D. Vittet, O. Feraud, R. Moore, R. Kemler, P. Huber, N-cadherin deficiency impairs pericyte recruitment, and not endothelial differentiation or sprouting, in embryonic stem cell-derived angiogenesis, Exp. Cell Res. 310 (2005) 392–400.

Drug Metab. Pharmacokinet. 29 (1): 44–51 (2014).

Regular Article

Differentiation of Human Induced Pluripotent Stem Cells into Functional Enterocyte-like Cells Using a Simple Method

Takahiro Iwao[1], Masashi Toyota[2], Yoshitaka Miyagawa[3], Hajime Okita[3], Nobutaka Kiyokawa[3], Hidenori Akutsu[2], Akihiro Umezawa[2], Kiyoshi Nagata[4] and Tamihide Matsunaga[1,*]

[1]*Department of Clinical Pharmacy, Graduate School of Pharmaceutical Sciences, Nagoya City University, Nagoya, Japan*
[2]*Department of Reproductive Biology, National Research Institute for Child Health and Development, Tokyo, Japan*
[3]*Department of Hematology and Oncology Research, National Research Institute for Child Health and Development, Tokyo, Japan*
[4]*Department of Environmental and Health Science, Tohoku Pharmaceutical University, Sendai, Japan*

Full text of this paper is available at http://www.jstage.jst.go.jp/browse/dmpk

Summary: Human induced pluripotent stem (iPS) cells were differentiated into the endoderm using activin A and were then treated with fibroblast growth factor 2 (FGF2) for differentiation into intestinal stem cell-like cells. These immature cells were then differentiated into enterocyte-like cells using epidermal growth factor (EGF) in 2% fetal bovine serum (FBS). At the early stage of differentiation, mRNA expression of caudal type homeobox 2 (CDX2), a major transcription factor related to intestinal development and differentiation, and leucine-rich repeat-containing G-protein-coupled receptor 5 (LGR5), an intestinal stem cell marker, was markedly increased by treatment with FGF2. When cells were cultured in medium containing EGF and a low concentration of FBS, mRNAs of specific markers of intestinal epithelial cells, including sucrase–isomaltase, the intestinal oligopeptide transporter SLC15A1/peptide transporter 1 (PEPT1), and the major metabolizing enzyme CYP3A4, were expressed. In addition, sucrase–isomaltase protein expression and uptake of β-Ala-Lys-N-7-amino-4-methylcoumarin-3-acetic acid (β-Ala-Lys-AMCA), a fluorescence-labeled substrate of the oligopeptide transporter, were detected. These results demonstrate a simple and direct method for differentiating human iPS cells into functional enterocyte-like cells.

Keywords: human iPS cells; intestinal differentiation; enterocytes; pharmacokinetics; drug metabolizing enzymes; drug transporters

Introduction

The small intestine and liver play important roles in all aspects of pharmacokinetics, including drug disposition, drug metabolism, drug transport, drug interactions, and bioavailability. Because drug-metabolizing enzymes such as cytochrome P450 (CYP) and UDP-glucuronyltransferase (UGT) and drug transporters such as ATP-binding cassette (ABC) and solute carrier (SLC) transporters are appreciably expressed in the small intestinal epithelia,[1,2] it is necessary to estimate intestinal metabolism and absorption during the early stages of drug development. To this end, various *in vivo* and *in vitro* systems have been employed to assess the intestinal first-pass effect. However, extrapolation of experimental animal data to humans is often hampered by species differences, and primary human intestinal cells are rarely available. Therefore, a system that accurately and easily estimates intestinal membrane permeability and metabolism is urgently required.

Human induced pluripotent stem (iPS) cells can be generated by transducing reprogramming factors (OCT3/4, SOX2, KLF4, c-MYC) into somatic cells[3] and these cells share many characteristics of embryonic stem (ES) cells.[4] Human iPS cells are expected to be useful not only in regenerative medicine but also in pharmacokinetic and toxicokinetic drug development studies because their use is not as ethically regulated as that of human ES cells.

Received January 25, 2013; Accepted June 21, 2013
J-STAGE Advance Published Date: July 2, 2013, doi:10.2133/dmpk.DMPK-13-RG-005
**To whom correspondence should be addressed:* Tamihide Matsunaga, Ph.D., *Department of Clinical Pharmacy, Graduate School of Pharmaceutical Sciences, Nagoya City University, 3-1 Tanabe-dori, Mizuho-ku, Nagoya 467-8603, Japan. Tel. +81-52-836-3751, Fax. +81-52-836-3751, E-mail: tmatsu@phar.nagoya-cu.ac.jp.*
This work was supported, in part, by Grants-in-Aid from the Japan Society for the Promotion of Science (23390036), by a National Grant-in-Aid from Japanese Ministry of Health, Labor, and Welfare (H22-003), and by a Grant-in-Aid for Research in Nagoya City University.

Therefore, human iPS cells have been differentiated into various cell types, including pancreatic cells,[5,6] neuron cells,[7] cardiomyocytes,[8] and hepatocytes.[9-13]

A few studies report the differentiation of iPS cells into enterocytes. In particular, mouse iPS cells were differentiated into a gut-like organ following the formation of embryoid bodies (EBs),[14] and human iPS cells were differentiated into intestinal tissue using a culture method for intestinal crypt stem cells.[15] However, functional characteristics of drug transporters and drug-metabolizing enzymes of differentiated cells are almost entirely unexplored in these reports. Thus, whether differentiated intestinal tissue or organoids can be used in drug development studies, particularly studies of the absorbability and metabolic capacity of drugs, remains unclear.

The small intestinal epithelium comprises absorptive cells, goblet cells, endocrine cells, and Paneth cells. Several signaling pathways such as Notch, Wnt, phosphoinositide 3-kinase, and bone morphogenic protein signaling are associated with intestinal development.[16] Leucine-rich repeat-containing G-protein-coupled receptor 5 (LGR5) has been identified as an intestinal stem cell marker.[17] Indeed, this was also observed in mouse LGR5-positive cells that formed a crypt–villus structure *in vitro*.[18] Improvements in this technique have enabled long-term culture of human epithelial cells isolated from the small intestine,[19] leading to advances in intestinal stem cell research. However, mechanisms of intestinal development are not sufficiently understood, and it is difficult to control differentiation into all four cell types.

In this study, we established a functional enterocyte-like cell line from human iPS cells for use in drug development studies. We propose a simple and direct differentiation method by two-dimensional culture. Our data may facilitate the development of an intestinal pharmacokinetic analysis system to identify safe drugs with favorable pharmacokinetic characteristics.

Materials and Methods

Materials: FGF2, FGF4, activin A, and epidermal growth factor (EGF) were purchased from PeproTech Inc. (Rocky Hill, NJ). Wnt3a was purchased from R&D Systems, Inc. (Minneapolis, MN). BD Matrigel matrix Growth Factor Reduced (Matrigel) was purchased from BD Biosciences (Bedford, MA). Affinity-isolated rabbit polyclonal antihuman sucrase–isomaltase antibody and intestinal recombinant protein epitope signature tags were purchased from Sigma-Aldrich Co. (St. Louis, MO). The purified IgG fraction of polyclonal goat antiserum against rabbit IgG conjugated with Alexa Fluor 568 and KnockOut Serum Replacement (KSR) were purchased from Invitrogen Life Technologies Co. (Carlsbad, CA). β-Ala-Lys-N-7-amino-4-methylcoumarin-3-acetic acid (β-Ala-Lys-AMCA) was purchased from BIOTREND Chemicals (Destin, FL), and (+)-(*R*)-*trans*-4-(1-aminoethyl)-*N*-(4-pyridyl)cyclohexanecarboxamide dihydrochloride (Y-27632) was purchased from Wako Pure Chemical Industries (Osaka, Japan). Human adult small intestine total RNA from a 66-year-old male donor was purchased from BioChain Institute Inc. (Newark, CA). Murine embryonic fibroblasts (MEFs) were obtained from Oriental Yeast Co. (Tokyo, Japan). The RNeasy Mini Kit was purchased from Qiagen (Valencia, CA). The PrimeScript RT Reagent Kit and TaKaRa SYBR Premix EX Taq II were purchased from Takara Bio Inc. (Otsu, Japan). All other reagents were of the highest quality available.

Human iPS cell cultures: A human iPS cell line (Windy) was provided by Dr. Akihiro Umezawa of the National Center for Child Health and Development. Human iPS cells were maintained in a 1:1 mixture of Dulbecco's modified Eagle's medium and Ham's nutrient mixture F-12 (DMEM/F12) containing 20% KSR, 2 mM L-glutamine, 1% MEM nonessential amino acid solution (NEAA), 0.1 mM 2-mercaptoethanol, and 5 ng/ml FGF2 at 37°C in humidified air with 5% CO_2. The human iPS cells were cultured on a feeder layer of mitomycin C-treated MEFs, and the medium was changed every day.

Differentiation into enterocyte-like cells: The human iPS cells were used for differentiation studies between passages 30 and 50. When the cells reached approximately 70% confluence, differentiation was initiated by replacing the medium with Rosewell Park Memorial Institute (RPMI) 1640 medium containing 2 mM GlutaMAX, 0.5% fetal bovine serum (FBS), 100 ng/ml activin A (a member of the transforming growth factor-β family that is known to efficiently induce differentiation into the definitive endoderm),[20,21] 100 units/ml penicillin, and 100 μg/ml streptomycin. After 48 h, the medium was replaced with RPMI 1640 containing 2 mM GlutaMAX, 2% FBS, 100 ng/ml activin A, 100 units/ml penicillin, and 100 μg/ml streptomycin, and the cells were cultured for 24 h. Subsequently, the culture medium was replaced with DMEM/F12 containing 2% FBS, 2 mM GlutaMAX, and 250 ng/ml FGF2 or FGF4 with or without 50 ng/ml Wnt3a for 96 h. The cells were then treated for 1 h with the selective Rho-associated kinase inhibitor Y-27632 at 10 μM.[22,23] The cells were then passaged on Matrigel-coated 24-well plates and cultured in DMEM/F12 containing 2% or 10% FBS, 2% B-27 supplement, 1% N2 supplement, 1% NEAA, 2 mM L-glutamine, antibiotics (100 units/ml penicillin and 100 μg/ml streptomycin), and 20 ng/ml EGF for 1, 4, 13, or 19 days. Y-27632 was added at 10 μM during the initial 24 h of culture. The medium was changed every 3 days (**Fig. 1**).

RNA extraction and reverse transcription reaction: Total RNA was isolated from differentiated iPS cells using the RNeasy Mini Kit. First-strand cDNA was prepared from 500 ng of total RNA. The reverse transcription reaction was performed using the PrimeScript RT Reagent Kit according to the manufacturer's instructions.

Real-time polymerase chain reaction (PCR) analysis: Relative mRNA expression levels were determined using SYBR Green real-time quantitative reverse transcription-PCR (RT-PCR). Real-time PCR analysis was performed on the Applied Biosystems 7300 Real Time PCR System using 7300 System SDS software version 1.4 (Applied Biosystems, Carlsbad, CA). PCR was performed with the primer pairs listed in **Table 1** using SYBR Premix EX Taq II. mRNA expression levels were normalized relative to that of the housekeeping gene glyceraldehyde-3-phosphate dehydrogenase (GAPDH).

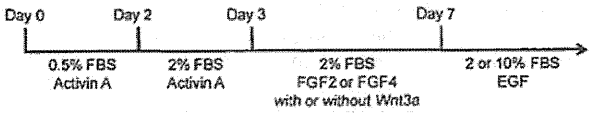

Fig. 1. Schematic of the protocol for the differentiation of human iPS cells into enterocytes
Human iPS cells were cultured in the presence of activin A (100 ng/ml) for 3 days. The cells were further cultured in medium containing FGF2 (250 ng/ml) or FGF4 (250 ng/ml) with or without Wnt3a (50 ng/ml) for 4 days. After 7 days of differentiation, the cells were treated with Y-27632 (10 μM), passaged, and subsequently cultured in the presence of 2% or 10% FBS and EGF (20 ng/ml) for 19 days.

Table 1. Sequences of primers for real-time PCR analysis

Gene name	Sense (5′→3′)	Antisense (5′→3′)	Product length (bp)
CDX2	ACCTGTGCGAGTGGATGC	TCCTTTGCTCTGCGGTTCT	232
LGR5	TGCTCTTCACCAACTGCATC	CTCAGGCTCACCAGATCCTC	193
DPP4	CAAATTGAAGCAGCCAGACA	GGAGTTGGGAGACCCATGTA	212
Sucrase-isomaltase	GGTAAGGAGAAACCGGGAAG	GCACGTCGACCTATGGAAAT	195
Villin 1	AGCCAGATCACTGCTGAGGT	TGGACAGGTGTTCCTCCTTC	169
ISX	CAGGAAGGAAGGAAGAGCAA	TGGGTAGTGGGTAAAGTGGAA	96
CYP3A4	CTGTGTGTTTCCAAGAGAAGTTAC	TGCATCAATTTCCTCCTGCAG	298
SLC15A1/PEPT1	CACCTCCTTGAAGAAGATGGCA	GGGAAGACTGGAAGAGTTTTATCG	105
SLC46A1/PCFT	GGTCTTTGCCTTTGCCACTA	AGAGTTTAGCCCGGATGACA	98
GAPDH	GAGTCAACGGATTTGGTCGT	GACAAGCTTCCCGTTCTCAG	185

Immunofluorescence staining: The cells differentiated with FGF2 and 2% FBS were washed three times with phosphate-buffered saline (PBS) without calcium or magnesium, fixed for 30 min at room temperature in 4% paraformaldehyde, and permeabilized in PBS containing 0.1% Triton X-100 for 5 min at room temperature. After being washed three times with PBS, the cells were blocked in PBS with 2% skim milk for 20 min at room temperature and were incubated with antisucrase-isomaltase antibody diluted at 1:200 for 60 min at room temperature. Rabbit serum was used as a negative control. The cells were washed three times with PBS and incubated with a 1:500 dilution of Alexa Fluor 568-labeled secondary antibody for 60 min at room temperature. After being washed three times with PBS, the cells were incubated with 1 μg/ml 4′,6-diamidino-2-phenylindole (DAPI) for 5 min at room temperature and washed with PBS. The cells were mounted on a glass slide using a 9:1 mixture of glycerol and PBS and viewed using an LSM 510Meta confocal microscope (Carl Zeiss Inc., Oberkochen, Germany).

Uptake study of β-Ala-Lys-AMCA: The cells differentiated with FGF2 and 2% FBS were rinsed several times with PBS and incubated with DMEM/F12 containing 25 μM β-Ala-Lys-AMCA for 4 h at 37°C. After incubation, uptake of β-Ala-Lys-AMCA was stopped by washing with ice-cold PBS. The cells were fixed for 30 min at room temperature in 4% paraformaldehyde, and immunofluorescence staining was performed using the primary and secondary antibodies as described above. The cells were then mounted using a 9:1 mixture of glycerol and PBS and viewed using an LSM 510Meta confocal microscope.

Statistical analysis: Levels of statistical significance were assessed using Student's *t*-test, and multiple comparisons were performed using analysis of variance (ANOVA) followed by Tukey's test.

Results

Early stages of differentiation into intestinal cells: For efficient, selective, and direct differentiation, a protocol designed to mimic intestinal development is desirable. We attempted differentiation into enterocytes that mediate the formation of the definitive endoderm. Because the intestine is an endoderm-derived organ, the human iPS cells were initially differentiated into the endoderm using a high concentration of activin A (100 ng/ml). Subsequently, we investigated the effects of FGF2, FGF4, and Wnt3a, which promote the development of mid- and hindgut lineages,[24,25] during differentiation from the definitive endoderm to intestinal stem cells. In these experiments, mRNA expression of caudal type homeobox 2 (CDX2), a major transcription factor of intestinal development and cell differentiation,[26,27] was slightly higher in FGF4-treated cells than that in FGF2-treated cells (**Fig. 2A**). In contrast, mRNA expression of LGR5 in FGF4-treated cells was significantly lower than that in FGF2-treated cells (**Fig. 2B**). Under all conditions, these mRNA expression levels were higher than those in undifferentiated human iPS cells. No effects of Wnt3a were observed on mRNA expression of CDX2 or LGR5 during the early stages of differentiation.

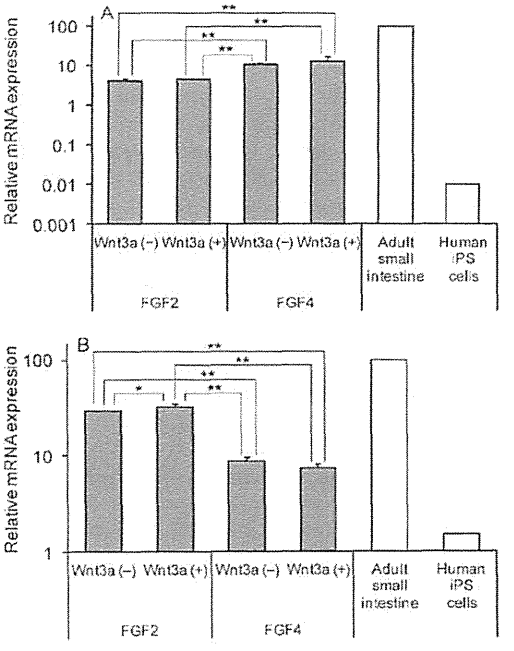

Fig. 2. Relative mRNA expression levels of CDX2 (A) and LGR5 (B) in differentiated intestinal stem cell-like cells
Human iPS cells were cultured in the presence of activin A for 3 days. The cells were further cultured in medium containing FGF2 or FGF4 with or without Wnt3a for 4 days and then in the presence of EGF for 1 day. After 8 days of differentiation, total RNA was extracted and mRNAs were analyzed by SYBR Green real-time RT-PCR. mRNA expression levels were normalized relative to that of GAPDH. Gene expression levels are represented relative to the level in the adult small intestine, which is set as 100. The adult small intestine and undifferentiated human iPS cells (shown as open columns) were used as positive and negative controls, respectively. Data are presented as the mean ± S.D. ($n = 3$), except for the adult small intestine and human iPS cells. Levels of statistical significance were compared among all groups: $^{**}p < 0.01$, $^{*}p < 0.05$.

Differentiation into enterocyte-like cells: To effectively differentiate human iPS cells into enterocyte-like cells, we examined

the effects of FBS concentration in the differentiation medium. Expression of LGR5 in differentiated human iPS cells did not differ in the presence of 2% or 10% FBS (**Fig. 3A**). However, mRNA expression of sucrase–isomaltase was 3.5-fold higher in 2% FBS than that in 10% FBS (**Fig. 3B**). In addition, mRNA expression levels of SLC15A1/peptide transporter 1 (PEPT1) and CYP3A4 were higher in the presence of 2% FBS (**Figs. 3C** and **3D**). In differentiated enterocyte-like cells, sucrase–isomaltase and CYP3A4, which were not detected in undifferentiated human iPS cells, were expressed, and mRNA expression levels of LGR5 and SLC15A1/PEPT1 were 30–40-fold higher than those in undifferentiated human iPS cells. Morphological changes in differentiating human iPS cells are shown in **Figure 4**. Similar to ES cells, undifferentiated human iPS cells had little cytoplasm and were small in size (**Fig. 4A**). When human iPS cells were cultured in the presence of activin A and FGF2, the cells gradually exhibited morphological changes such as enlargement and acquisition of spiky shapes (**Fig. 4B**). At the final stage of differentiation with EGF and 2% FBS, a number of dome-like structures formed and were assumed to contain liquids and cells (**Figs. 4C** and **4D**). In cells differentiated with activin A, FGF2, EGF, and 2% FBS, villin 1[28,29] and intestine specific homeobox (ISX)[30] were expressed, whereas intestinal fatty acid-binding protein (IFABP) was not expressed. Interestingly, mRNA expression levels of CDX2, dipeptidyl peptidase 4 (DPP4), and SLC46A1/proton-coupled folate transporter (PCFT) were similar to those in the adult small intestine, which was used as a positive control (**Fig. 5**). However, gene expression levels of UGT1A1 and ABCB1/multidrug resistance 1 (MDR1) were similar to those in undifferentiated human iPS cells (data not shown).

To determine the optimal duration of differentiation, we examined time-dependent variations in expression levels of specific small intestine genes such as LGR5, sucrase–isomaltase, and SLC15A1/PEPT1. After short-term culture (11 days), mRNA expression levels of sucrase–isomaltase and SLC15A1/PEPT1 were very low but gradually increased with differentiation until day 26. Similarly, CYP3A4 mRNA was not expressed after 11 days of differentiation but was expressed after 20 days (**Fig. 6**). LGR5 mRNA did not change with the duration of differentiation.

Immunofluorescence staining of sucrase–isomaltase in enterocyte-like cells: Sucrase–isomaltase is an essential carbohydrate digestion enzyme that is specifically expressed in brush border membranes of mature enterocytes. Therefore, sucrase–isomaltase expression is thought to be an indicator of differentiation into enterocytes. Indeed, protein expression of sucrase–isomaltase was confirmed in differentiated cells using immunofluorescence staining, in particular, in dense clusters of cells (**Fig. 7**).

Uptake of β-Ala-Lys-AMCA in enterocyte-like cells: Oligopeptide transporters are expressed in the brush border membrane and participate in peptide absorption from the intestinal lumen.[2] As shown in **Figure 3C**, expression of SLC15A1/PEPT1 mRNA in differentiated enterocyte-like cells was more than 30-fold higher than that in undifferentiated human iPS cells. To determine whether this leads to active peptide transport in differentiated cells, we performed peptide uptake assays using β-Ala-Lys-AMCA, a fluorescence-labeled substrate of the oligopeptide transporter.[31] As shown in **Figure 8**, intracellular uptake of β-Ala-Lys-AMCA was observed in cells expressing the sucrase–isomaltase proteins. However, uptake of β-Ala-Lys-AMCA at 4°C was low compared with that at 37°C (data not shown).

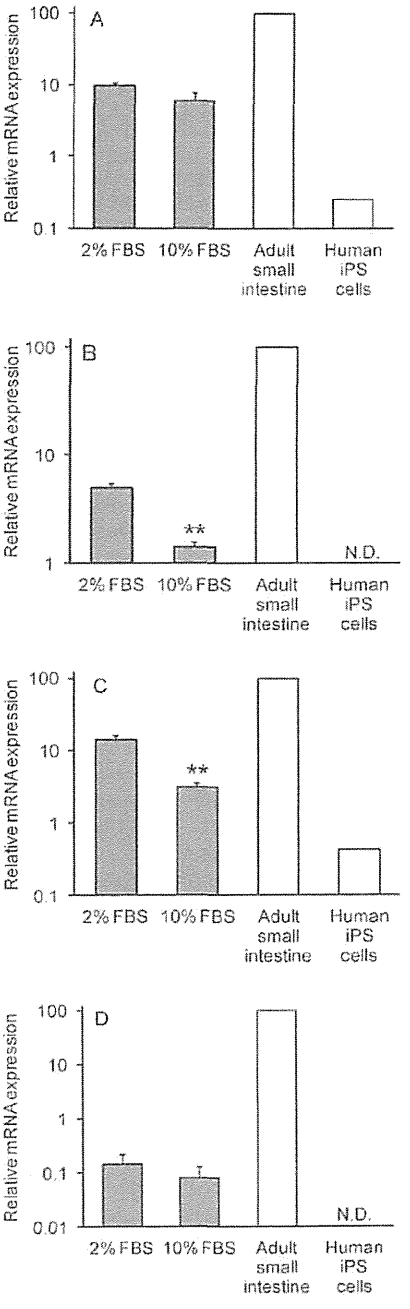

Fig. 3. Relative mRNA expression levels of LGR5 (A), sucrase–isomaltase (B), SLC15A1/PEPT1 (C), and CYP3A4 (D) in differentiated enterocyte-like cells cultured in 2% or 10% FBS

Human iPS cells were cultured in the presence of activin A for 3 days. The cells were further cultured in medium containing FGF2 for 4 days and then in the presence of 2% or 10% FBS and EGF for 17 days. After 24 days of differentiation, total RNA was extracted and mRNAs were analyzed by SYBR Green real-time RT-PCR. mRNA expression levels were normalized relative to that of GAPDH. Gene expression levels are represented relative to the level in the adult small intestine, which is set as 100. The adult small intestine and undifferentiated human iPS cells (shown as open columns) were used as positive and negative controls, respectively. Data are presented as the mean ± S.D. ($n = 3$), except for the adult small intestine and human iPS cells. N.D., not detected. Levels of statistical significance were compared with the 2% FBS group: $^{**}p < 0.01$.

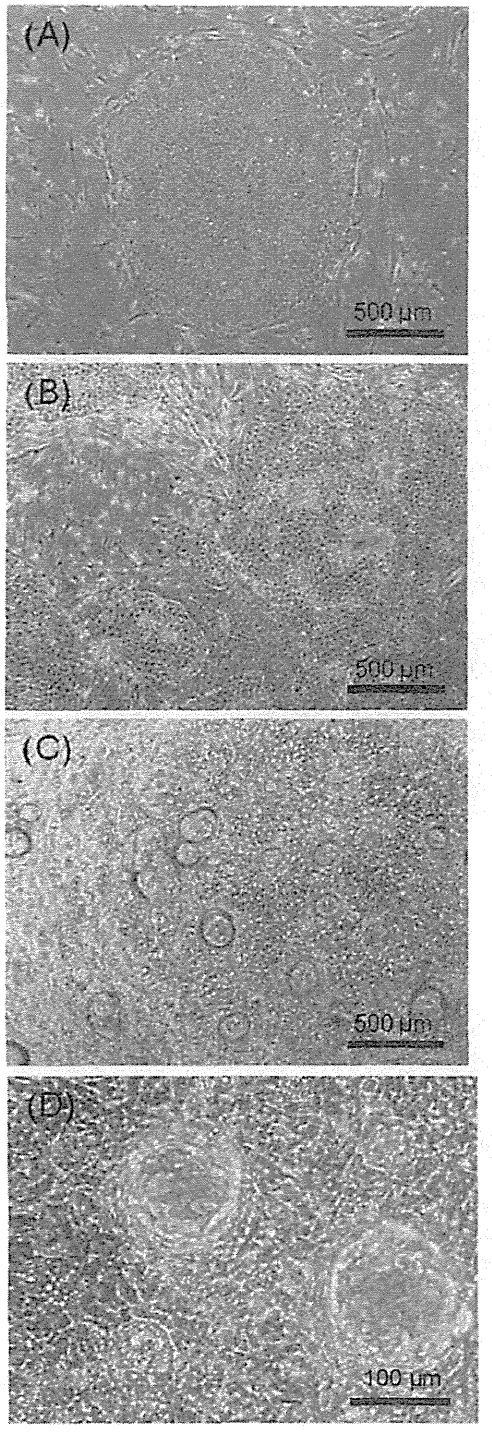

Fig. 4. Morphological changes in human iPS cells during differentiation into enterocyte-like cells
Human iPS cells were cultured in medium containing activin A for 3 days, FGF2 for 4 days, and 2% FBS and EGF for 17 days. (A) Undifferentiated human iPS cells; (B) midgut lineage cell-like cells after 7 days of differentiation; (C, D) enterocyte-like cells after 24 days of differentiation. Scale bar, 500 μm (A–C), 100 μm (D).

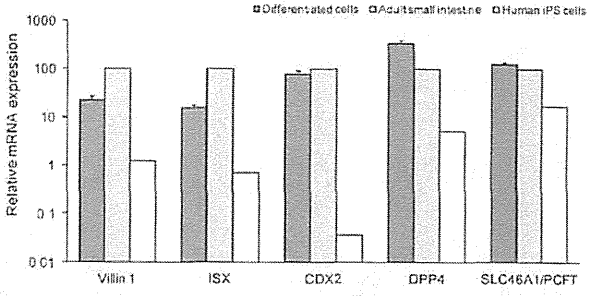

Fig. 5. Relative mRNA expression levels of the intestinal markers villin 1, ISX, CDX2, DPP4, and SLC46A1/PCFT in differentiated enterocyte-like cells
Human iPS cells were cultured in the presence of activin A for 3 days. The cells were further cultured in medium containing FGF2 for 4 days and then in the presence of 2% FBS and EGF for 19 days. After 26 days of differentiation, total RNA was extracted and mRNAs were analyzed by SYBR Green real-time RT-PCR. mRNA expression levels were normalized relative to that of GAPDH. Gene expression levels are represented relative to the level in the adult small intestine, which is set as 100. The adult small intestine and undifferentiated human iPS cells (shown as open columns) were used as positive and negative controls, respectively. Data are presented as the mean ± S.D. ($n = 3$), except for the adult small intestine and human iPS cells.

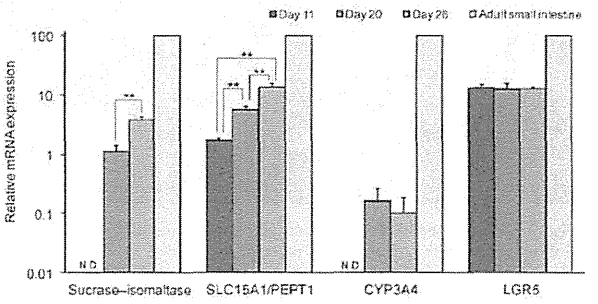

Fig. 6. Time-dependent variation in mRNA expression levels of sucrase–isomaltase, SLC15A1/PEPT1, CYP3A4, and LGR5 in differentiated enterocyte-like cells
Human iPS cells were cultured in the presence of activin A for 3 days. The cells were further cultured in medium containing FGF2 for 4 days and then in the presence of 2% FBS and EGF for 4, 13, or 19 days. After 11, 20, or 26 days of differentiation, total RNA was extracted and mRNAs were analyzed by SYBR Green real-time RT-PCR. mRNA expression levels were normalized relative to that of GAPDH. Gene expression levels are represented relative to the level in the adult small intestine, which is set as 100. The adult small intestine was used as a positive control. Data are presented as the mean ± S.D. ($n = 4$) except for the adult small intestine. N.D., not detected. Levels of statistical significance were compared among all groups: $^{**}p < 0.01$.

Discussion

Ueda *et al.*[14] reported the synthesis of gut-like organs from mouse iPS cells using the EB formulation technique with mouse ES cells. However, this hanging drop culture technique is hampered by its high requirement of skill, low EB formulation efficiency, unstable EB quality, and differing differentiation efficiencies between EBs. Spence *et al.*[15] reported the direct differentiation of human iPS cells into three-dimensional intestinal organoids. These organoids contained various cell types, including enterocytes, endocrine cells, goblet cells, and Paneth cells, although expression of drug-metabolizing enzymes and transporters, which are central to drug absorption and metabolism, was not examined. In their study, the intestinal crypt culture system, in which spheroids

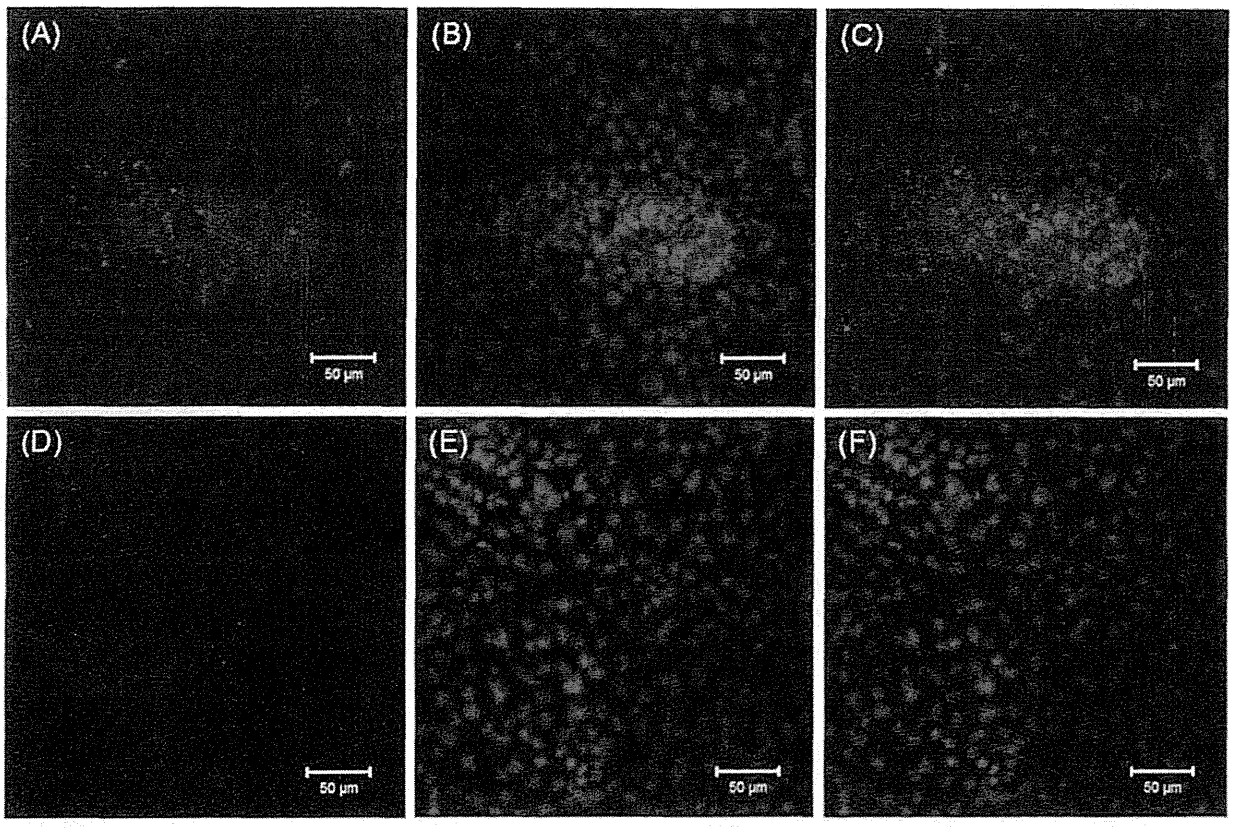

Fig. 7. Immunofluorescence analysis of sucrase–isomaltase in differentiated enterocyte-like cells
Human iPS cells were cultured in the presence of activin A for 3 days. The cells were further cultured in medium containing FGF2 for 4 days and then in the presence of 2% FBS and EGF for 19 days. After 26 days of differentiation, differentiated cells were stained with antisucrase–isomaltase antibody (A–C) or nonimmune rabbit serum as a negative control (D–F). Nuclei were counterstained with DAPI. (A) Immunofluorescence staining of sucrase–isomaltase (red); (D) immunofluorescence staining of rabbit serum as a negative control; (B, E) DAPI-stained DNA (blue); (C, F) overlay (Merge) image of sucrase–isomaltase and DAPI. Scale bar, 50 μm.

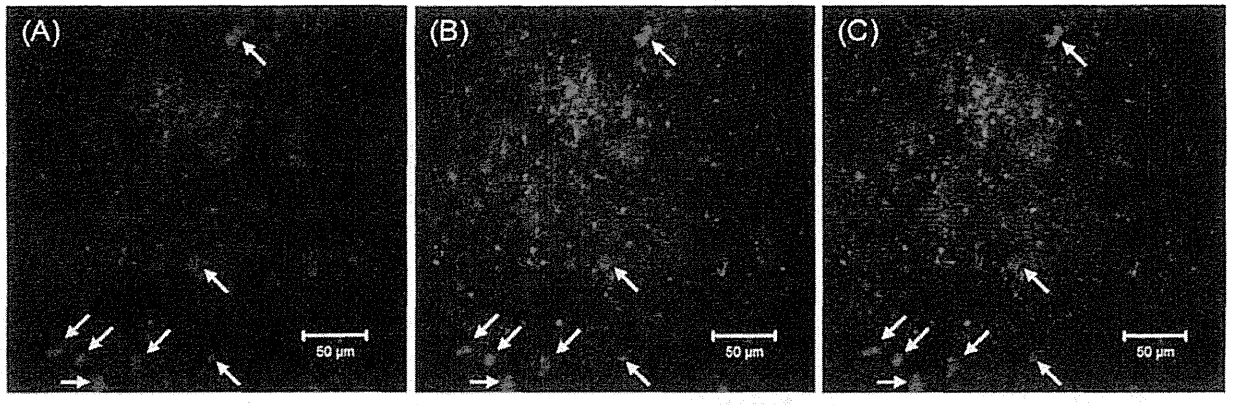

Fig. 8. Uptake of β-Ala-Lys-AMCA into differentiated enterocyte-like cells
Human iPS cells were cultured in the presence of activin A for 3 days. The cells were further cultured in medium containing FGF2 for 4 days and then in the presence of 2% FBS and EGF for 19 days. After 26 days of differentiation, the differentiated cells were incubated with β-Ala-Lys-AMCA (25 μM) for 4 h at 37°C. After uptake was stopped, the differentiated cells were fixed and stained with antisucrase–isomaltase antibody. Typical images from β-Ala-Lys-AMCA uptake experiments. Arrows indicate co-localization of β-Ala-Lys-AMCA and sucrase–isomaltase protein. (A) Intracellular uptake of β-Ala-Lys-AMCA (blue); (B) immunofluorescence staining of sucrase–isomaltase (red); (C) overlay (Merge) image of β-Ala-Lys-AMCA and sucrase–isomaltase. Scale bar, 50 μm.

are formed by three-dimensional culture, was applied during differentiation from the endoderm to intestinal organoids, and several factors were added in large quantities to induce differentiation. This method may be suitable for the culture of intestinal stem cells but not for selective differentiation into enterocytes, and it is complicated and costly. Therefore, we generated enterocyte-like cells using a simple two-dimensional culture method.

Spence *et al.*[15] also reported that the combination of FGF4 (500 ng/ml) and Wnt3a (500 ng/ml) effectively posteriorized the endoderm. Ameri *et al.*[32] reported the induction of CDX2 with FGF2 (256 ng/ml) in a concentration-dependent manner in the human ES cell-derived endoderm. In the present study, we examined the effects of FGF2, FGF4, and Wnt3a on the induction of the midgut endoderm lineage. Our results showed that the expression level of CDX2 was comparable in the FGF2 and FGF4 treatment groups, whereas no effect of Wnt3a was observed. These results were inconsistent with those of Spence *et al.*,[15] possibly because of the lower concentrations of Wnt3a used in our study (50 ng/ml). Sherwood *et al.*[33] demonstrated that β-catenin-dependent Wnt signaling, activated by the glycogen synthase kinase-3 (GSK3) inhibitor, induced the expression of the intestinal master regulator Cdx2 and induced intestinal differentiation of the ES cell-derived endoderm and large intestinal gene expression. They also indicated that because of poor bioactivity, the induction level of Cdx2 expression by Wnt3a was lower than that by the GSK3 inhibitor. Therefore, superior stability and bioactivity of small-molecule compounds may lead to more effective experimental regulation of these signaling pathways. However, the striking activation of Wnt signaling also induced large intestinal gene expression, and further investigations of the extent of activation of Wnt signaling during small intestinal differentiation may be required. The expression of LGR5[17] was higher in the FGF2 treatment group than that in the FGF4 treatment group. Therefore, subsequent differentiation experiments were performed using FGF2.

We have demonstrated that enterocyte-like cells, which express the specific intestinal markers sucrase–isomaltase,[34,35] villin 1, ISX, and pharmacokinetics-related genes, were differentiated from an intestinal stem cell-like cell population by two-dimensional culture with EGF and a low serum concentration. Sucrase–isomaltase and SLC15A1/PEPT1 mRNA gradually increased with the duration of differentiation, indicating that longer duration may be necessary to efficiently obtain mature enterocytes. In contrast, LGR5 mRNA expression remained unchanged, suggesting that enterocytes matured during intestinal stem cell proliferation. DPP4 (serine protease) and SLC46A1/PCFT (folate transporter) are known to be abundantly expressed in epithelial cells of the small intestine.[36,37] Expression of DPP4 and SLC46A1/PCFT in differentiated cells was higher than that in adult small intestine samples. Intestinal differentiation was promoted by low FBS concentrations in this study. Potentially, the growth of extra-enterocytic cells such as fibroblasts may be suppressed with decreasing FBS concentrations, and some differentiation and growth-inhibiting factors may be present in FBS, although the mechanisms underlying these effects remain unclear.

At present, human intestinal epithelial cells are difficult to obtain, and no appropriate model cell system exists. Instead, other tissue cell-derived cell lines, including Caco-2 cells (human colon carcinoma cell line) and Madin–Darby canine kidney (MDCK) cells, have been used as intestinal models in drug absorption studies.[2,38] However, drug transporter expression patterns in these cells considerably differ from those in enterocytes. In particular, CYP3A4 is expressed at very low levels in these cell lines. In the present study, cells expressing the sucrase–isomaltase protein showed uptake of β-Ala-Lys-AMCA, the substrate of the oligopeptide transporter (**Fig. 8**). Differentiated cells also expressed CYP3A4 mRNA, albeit at levels lower than those in the adult small intestine (**Fig. 3**), suggesting that enterocyte-like cells differentiated from human iPS cells have peptide-transporting activity and may be useful in the study of drug absorbability.

In this study, we used a human iPS cell line, which is easily differentiated into hepatocytes of an endodermal lineage, because the intestine is also an endoderm-derived tissue. Differentiation propensity is known to be markedly different among human ES and iPS cell lines.[39,40] Thus, there may be a difference in the degree of intestinal differentiation depending on the human iPS cell line being tested. Regarding this point, we believe it is necessary to perform studies comparing intestinal differentiation among human iPS cell lines in the future.

In conclusion, because the intestine is an endoderm-derived tissue, human iPS cells were directly differentiated into the endoderm using activin A. Subsequently, we devised a simple method for differentiation into enterocyte-like cells with functional peptide transport by two-dimensional culture and the addition of several growth factors. These data suggest that human iPS-derived enterocytes may facilitate future drug development studies. If enterocyte-like cells, which have functional features similar to those of enterocytes, can be generated from human iPS cells, it may be possible to construct systems for easy estimation of overall intestinal function, including absorption and metabolism.

References

1) Paine, M. F., Hart, H. L., Ludington, S. S., Haining, R. L., Rettie, A. E. and Zeldin, D. C.: The human intestinal cytochrome P450 'pie'. *Drug Metab. Dispos.*, **34**: 880–886 (2006).
2) Giacomini, K. M., Huang, S.-M., Tweedie, D. J., Benet, L. Z., Brouwer, K. L. R., Chu, X., Dahlin, A., Evers, R., Fischer, V., *et al.*: Membrane transporters in drug development. *Nat. Rev. Drug Discov.*, **9**: 215–236 (2010).
3) Takahashi, K., Tanabe, K., Ohnuki, M., Narita, M., Ichisaka, T., Tomoda, K. and Yamanaka, S.: Induction of pluripotent stem cells from adult human fibroblasts by defined factors. *Cell*, **131**: 861–872 (2007).
4) Ochiya, T., Yamamoto, Y. and Banas, A.: Commitment of stem cells into functional hepatocytes. *Differentiation*, **79**: 65–73 (2010).
5) Tateishi, K., He, J., Taranova, O., Liang, G., D'Alessio, A. C. and Zhang, Y.: Generation of insulin-secreting islet-like clusters from human skin fibroblasts. *J. Biol. Chem.*, **283**: 31601–31607 (2008).
6) Zhang, D., Jiang, W., Liu, M., Sui, X., Yin, X., Chen, S., Shi, Y. and Deng, H.: Highly efficient differentiation of human ES cells and iPS cells into mature pancreatic insulin-producing cells. *Cell Res.*, **19**: 429–438 (2009).
7) Chambers, S. M., Fasano, C. A., Papapetrou, E. P., Tomishima, M., Sadelain, M. and Studer, L.: Highly efficient neural conversion of human ES and iPS cells by dual inhibition of SMAD signaling. *Nat. Biotechnol.*, **27**: 275–280 (2009).
8) Zhang, J., Wilson, G. F., Soerens, A. G., Koonce, C. H., Yu, J., Palecek, S. P., Thomson, J. A. and Kamp, T. J.: Functional cardiomyocytes derived from human induced pluripotent stem cells. *Circ. Res.*, **104**: e30–e41 (2009).
9) Song, Z., Cai, J., Liu, Y., Zhao, D., Yong, J., Duo, S., Song, X., Guo, Y., Zhao, Y., *et al.*: Efficient generation of hepatocyte-like cells from human induced pluripotent stem cells. *Cell Res.*, **19**: 1233–1242 (2009).
10) Sullivan, G. J., Hay, D. C., Park, I.-H., Fletcher, J., Hannoun, Z., Payne, C. M., Dalgetty, D., Black, J. R., Ross, J. A., *et al.*: Generation of functional human hepatic endoderm from human induced pluripotent stem cells. *Hepatology*, **51**: 329–335 (2010).
11) Si-Tayeb, K., Noto, F. K., Nagaoka, M., Li, J., Battle, M. A., Duris, C., North, P. E., Dalton, S. and Duncan, S. A.: Highly efficient generation of human hepatocyte-like cells from induced pluripotent stem cells.

Hepatology, **51**: 297–305 (2010).
12) Touboul, T., Hannan, N. R. F., Corbineau, S., Martinez, A., Martinet, C., Branchereau, S., Mainot, S., Strick-Marchand, H., Pedersen, R., *et al.*: Generation of functional hepatocytes from human embryonic stem cells under chemically defined conditions that recapitulate liver development. *Hepatology*, **51**: 1754–1765 (2010).
13) Takayama, K., Inamura, M., Kawabata, K., Tashiro, K., Katayama, K., Sakurai, F., Hayakawa, T., Furue, M. K. and Mizuguchi, H.: Efficient and directive generation of two distinct endoderm lineages from human ESCs and iPSCs by differentiation stage-specific SOX17 transduction. *PLoS ONE*, **6**: e21780 (2011).
14) Ueda, T., Yamada, T., Hokuto, D., Koyama, F., Kasuda, S., Kanehiro, H. and Nakajima, Y.: Generation of functional gut-like organ from mouse induced pluripotent stem cells. *Biochem. Biophys. Res. Commun.*, **391**: 38–42 (2010).
15) Spence, J. R., Mayhew, C. N., Rankin, S. A., Kuhar, M. F., Vallance, J. E., Tolle, K., Hoskins, E. E., Kalinichenko, V. V., Wells, S. I., *et al.*: Directed differentiation of human pluripotent stem cells into intestinal tissue in vitro. *Nature*, **470**: 105–109 (2011).
16) Scoville, D. H., Sato, T., He, X. C. and Li, L.: Current view: intestinal stem cells and signaling. *Gastroenterology*, **134**: 849–864 (2008).
17) Barker, N., van Es, J. H., Kuipers, J., Kujala, P., van den Born, M., Cozijnsen, M., Haegebarth, A., Korving, J., Begthel, H., *et al.*: Identification of stem cells in small intestine and colon by marker gene Lgr5. *Nature*, **449**: 1003–1007 (2007).
18) Sato, T., Vries, R. G., Snippert, H. J., van de Wetering, M., Barker, N., Stange, D. E., van Es, J. H., Abo, A., Kujala, P., *et al.*: Single Lgr5 stem cells build crypt-villus structures in vitro without a mesenchymal niche. *Nature*, **459**: 262–265 (2009).
19) Sato, T., Stange, D. E., Ferrante, M., Vries, R. G. J., van Es, J. H., van den Brink, S., van Houdt, W. J., Pronk, A., van Gorp, J., *et al.*: Long-term expansion of epithelial organoids from human colon, adenoma, adenocarcinoma, and Barrett's epithelium. *Gastroenterology*, **141**: 1762–1772 (2011).
20) D'Amour, K. A., Agulnick, A. D., Eliazer, S., Kelly, O. G., Kroon, E. and Baetge, E. E.: Efficient differentiation of human embryonic stem cells to definitive endoderm. *Nat. Biotechnol.*, **23**: 1534–1541 (2005).
21) McLean, A. B., D'Amour, K. A., Jones, K. L., Krishnamoorthy, M., Kulik, M. J., Reynolds, D. M., Sheppard, A. M., Liu, H., Xu, Y., *et al.*: Activin A efficiently specifies definitive endoderm from human embryonic stem cells only when phosphatidylinositol 3-kinase signaling is suppressed. *Stem Cells*, **25**: 29–38 (2007).
22) Ishizaki, T., Uchata, M., Tamechika, I., Keel, J., Nonomura, K., Maekawa, M. and Narumiya, S.: Pharmacological properties of Y-27632, a specific inhibitor of rho-associated kinases. *Mol. Pharmacol.*, **57**: 976–983 (2000).
23) Watanabe, K., Ueno, M., Kamiya, D., Nishiyama, A., Matsumura, M., Wataya, T., Takahashi, J. B., Nishikawa, S., Nishikawa, S., *et al.*: A ROCK inhibitor permits survival of dissociated human embryonic stem cells. *Nat. Biotechnol.*, **25**: 681–686 (2007).
24) Dessimoz, J., Opoka, R., Kordich, J. J., Grapin-Botton, A. and Wells, J. M.: FGF signaling is necessary for establishing gut tube domains along the anterior–posterior axis in vivo. *Mech. Dev.*, **123**: 42–55 (2006).
25) McLin, V. A., Rankin, S. A. and Zorn, A. M.: Repression of Wnt/β-catenin signaling in the anterior endoderm is essential for liver and pancreas development. *Development*, **134**: 2207–2217 (2007).
26) Escaffit, F., Paré, F., Gauthier, R., Rivard, N., Boudreau, F. and Beaulieu, J.-F.: Cdx2 modulates proliferation in normal human intestinal epithelial crypt cells. *Biochem. Biophys. Res. Commun.*, **342**: 66–72 (2006).
27) Gao, N., White, P. and Kaestner, K. H.: Establishment of intestinal identity and epithelial-mesenchymal signaling by Cdx2. *Dev. Cell*, **16**: 588–599 (2009).
28) Robine, S., Huet, C., Moll, R., Sahuquillo-Merino, C., Coudrier, E., Zweibaum, A. and Louvard, D.: Can villin be used to identify malignant and undifferentiated normal digestive epithelial cells? *Proc. Natl. Acad. Sci. USA*, **82**: 8488–8492 (1985).
29) Boller, K., Arpin, M., Pringault, E., Mangeat, P. and Reggio, H.: Differential distribution of villin and villin mRNA in mouse intestinal epithelial cells. *Differentiation*, **39**: 51–57 (1988).
30) Seino, Y., Miki, T., Kiyonari, H., Abe, T., Fujimoto, W., Kimura, K., Takeuchi, A., Takahashi, Y., Oiso, Y., *et al.*: Isx participates in the maintenance of vitamin A metabolism by regulation of beta-carotene 15,15'-monooxygenase (Bcmo1) expression. *J. Biol. Chem.*, **283**: 4905–4911 (2008).
31) Groneberg, D. A., Döring, F., Eynott, P. R., Fischer, A. and Daniel, H.: Intestinal peptide transport: ex vivo uptake studies and localization of peptide carrier PEPT1. *Am. J. Physiol. Gastrointest. Liver Physiol.*, **281**: G697–G704 (2001).
32) Ameri, J., Ståhlberg, A., Pedersen, J., Johansson, J. K., Johannesson, M. M., Artner, I. and Semb, H.: FGF2 specifies hESC-derived definitive endoderm into foregut/midgut cell lineages in a concentration-dependent manner. *Stem Cells*, **28**: 45–56 (2010).
33) Sherwood, R. I., Maehr, R., Mazzoni, E. O. and Melton, D. A.: Wnt signaling specifies and patterns intestinal endoderm. *Mech. Dev.*, **128**: 387–400 (2011).
34) Boudreau, F., Rings, E. H. H. M., van Wering, H. M., Kim, R. K., Swain, G. P., Krasinski, S. D., Moffett, J., Grand, R. J., Suh, E. R., *et al.*: Hepatocyte nuclear factor-1α, GATA-4, and caudal related homeodomain protein Cdx2 interact functionally to modulate intestinal gene transcription. *J. Biol. Chem.*, **277**: 31909–31917 (2002).
35) Gu, N., Adachi, T., Matsunaga, T., Tsujimoto, G., Ishihara, A., Yasuda, K. and Tsuda, K.: HNF-1α participates in glucose regulation of sucrase-isomaltase gene expression in epithelial intestinal cells. *Biochem. Biophys. Res. Commun.*, **353**: 617–622 (2007).
36) Qiu, A., Jansen, M., Sakaris, A., Min, S. H., Chattopadhyay, S., Tsai, E., Sandoval, C., Zhao, R., Akabas, M. H., *et al.*: Identification of an intestinal folate transporter and the molecular basis for hereditary folate malabsorption. *Cell*, **127**: 917–928 (2006).
37) Darmoul, D., Voisin, T., Couvineau, A., Rouyer-Fessard, C., Salomon, R., Wang, Y., Swallow, D. M. and Laburthe, M.: Regional expression of epithelial dipeptidyl peptidase IV in the human intestines. *Biochem. Biophys. Res. Commun.*, **203**: 1224–1229 (1994).
38) Volpe, D. A.: Drug-permeability and transporter assays in Caco-2 and MDCK cell lines. *Future Med. Chem.*, **3**: 2063–2077 (2011).
39) Osafune, K., Caron, L., Borowiak, M., Martinez, R. J., Fitz-Gerald, C. S., Sato, Y., Cowan, C. A., Chien, K. R. and Melton, D. A.: Marked differences in differentiation propensity among human embryonic stem cell lines. *Nat. Biotechnol.*, **26**: 313–315 (2008).
40) Kajiwara, M., Aoi, T., Okita, K., Takahashi, R., Inoue, H., Takayama, N., Endo, H., Eto, K., Toguchida, J., *et al.*: Donor-dependent variations in hepatic differentiation from human-induced pluripotent stem cells. *Proc. Natl. Acad. Sci. USA*, **109**: 12538–12543 (2012).

PLOS | ONE

β-Catenin Functions Pleiotropically in Differentiation and Tumorigenesis in Mouse Embryo-Derived Stem Cells

Noriko Okumura[2], Hidenori Akutsu[1]*, Tohru Sugawara[1], Takumi Miura[1], Youki Takezawa[1], Akihiro Hosoda[1], Keiichi Yoshida[1], Justin K. Ichida[3], Mitsutoshi Yamada[2], Toshio Hamatani[2], Naoaki Kuji[2], Kenji Miyado[1], Yasunori Yoshimura[2], Akihiro Umezawa[1]

1 Department of Reproductive Biology, National Center for Child Health and Development, Tokyo, Japan, **2** Department of Obstetrics and Gynecology, Keio University School of Medicine, Tokyo, Japan, **3** Department of Stem Cell and Regenerative Biology, Harvard University, Cambridge, Massachusetts, United States of America

Abstract

The canonical Wnt/β-catenin signaling pathway plays a crucial role in the maintenance of the balance between proliferation and differentiation throughout embryogenesis and tissue homeostasis. β-Catenin, encoded by the *Ctnnb1* gene, mediates an intracellular signaling cascade activated by Wnt. It also plays an important role in the maintenance of various types of stem cells including adult stem cells and cancer stem cells. However, it is unclear if β-catenin is required for the derivation of mouse embryo-derived stem cells. Here, we established β-catenin-deficient (β-cat$^{\Delta/\Delta}$) mouse embryo-derived stem cells and showed that β-catenin is not essential for acquiring self-renewal potential in the derivation of mouse embryonic stem cells (ESCs). However, teratomas formed from embryo-derived β-cat$^{\Delta/\Delta}$ ESCs were immature germ cell tumors without multilineage differentiated cell types. Re-expression of functional β-catenin eliminated their neoplastic, transformed phenotype and restored pluripotency, thereby rescuing the mutant ESCs. Our findings demonstrate that β-catenin has pleiotropic effects in ESCs; it is required for the differentiation of ESCs and prevents them from acquiring tumorigenic character. These results highlight β-catenin as the gatekeeper in differentiation and tumorigenesis in ESCs.

Citation: Okumura N, Akutsu H, Sugawara T, Miura T, Takezawa Y, et al. (2013) β-Catenin Functions Pleiotropically in Differentiation and Tumorigenesis in Mouse Embryo-Derived Stem Cells. PLoS ONE 8(5): e63265. doi:10.1371/journal.pone.0063265

Editor: Masaru Katoh, National Cancer Center, Japan

Received November 16, 2012; **Accepted** April 1, 2013; **Published** May 14, 2013

Funding: This work was supported by grants from the Ministry of Education, Culture, Sports, Science and Technology (MEXT) of Japan; a grant from the Ministry of Health, Labour and Welfare (MHLW) to HA, AU; a Grant-in-aid for Scientific Research (21390456) to HA, and (22770233) to TS; a grant from JST-CREST given to HA. The funders had no control over the study design, data collection and analysis, decision to publish, or preparation of the manuscript.

Competing Interests: The authors have declared that no competing interests exist.

* E-mail: akutsu-h@ncchd.go.jp

Introduction

The Wnt/β-catenin signaling pathway is an evolutionarily conserved signal transduction cascade and functions during early development to regulate body axis specification, germ layer formation and organogenesis [1]. It is not surprising that mutations of the Wnt pathway components are associated with many hereditary disorders, cancer, and other diseases [2]. In preimplantation embryo development, fertilized oocytes go through a series of cleavage divisions which lead to blastocyst formation. The body axes and germ layers in mammalian embryos are established after implantation and Wnt/β-catenin signaling plays an important role in the establishment of the basic body plan in mouse embryos [1]. Embryonic stem cells (ESCs) are derived from the inner cell mass (ICM) of the mammalian blastocyst and are capable of proliferating indefinitely in culture while maintaining an undifferentiated pluripotent state [3,4]. Wnt/β-Catenin signaling has a dominant role in the *in vitro* maintenance of both mouse and human ESCs [5]. However, it is unclear how the known function of Wnt signaling in early embryonic development relates to its regulation of pluripotency and lineage decisions in pluripotent stem cells.

β-Catenin is an essential component of the Wnt/β-catenin signaling pathway. In the absence of a Wnt signal, β-catenin is rapidly degraded by a multi-protein complex including Axin, adenomatous polyposis coli (APC) and glycogen synthase kinase 3 (GSK3). Wnt proteins stimulate signaling through various frizzled receptors, low density lipoprotein receptor-related protein 5/6 (LRP 5/6) co-receptors and disheveled to inactivate the β-catenin-degradation complex, and the stabilized β-catenin associates with transcription factors of the Tcf (T-cell factor)/Lef (lymphoid enhancer factor) family resulting in the transcriptional activation of target genes [1,5].

Previous studies based on both loss- and gain-of-function mutations of β-catenin in mice have established the importance of the role of Wnt/β-catenin signaling in the regulation of the vertebral axis, germ layer specification and tumorigenesis [6]. Elegant studies have genetically demonstrated that β-catenin is indispensable for differentiation, but it is not required for self-renewal of mouse ESCs [7,8]. The *Ctnnb1* deficient mouse ESC lines were established by deleting functional exons in cultured mouse ESC lines, and it still remains to be determined whether β-catenin plays an important role in the transformation of preimplantation embryos into pluripotent stem cells.

Our recent work demonstrated that β-catenin plays a role in sperm-oocyte membrane adhesion and the transition of the membrane upon mouse fertilization, using homogenous defects of β-catenin in both oocyte and sperm cells [9]. Here, we report the generation of novel Ctnnb1-deficient mouse embryo-derived stem cells (β-cat$^{\Delta/\Delta}$ mESCs) with the deletion of exons 2–6 using

mice containing the loss-of-function mutation in β-catenin to produce mutant oocyte and sperm through the germ cell-specific Cre-loxP system. β-cat$^{\Delta/\Delta}$ mESCs are a material which can be used to address the role of β-catenin in the acquisition of pluripotency including self-renewal and differentiation from preimplantation embryos. It is also noteworthy that β-cat$^{\Delta/\Delta}$ mESCs lack the residual β-catenin of either maternal or paternal origin. Our results show that β-catenin is not essential for acquiring and maintaining proliferative self-renewal, but that it is required for normal multilineage differentiation. Interestingly, these embryo-derived β-cat$^{\Delta/\Delta}$ mESCs contributed to oncogenic germ cell tumors in a teratoma assay. These results were corroborated by our rescued β-cat$^{\Delta/\Delta}$ mESCs experiments. Our findings show that β-catenin plays an important role in multilineage differentiation and tumorigenesis in germ cell tumors. Our embryo-derived β-cat$^{\Delta/\Delta}$ mESCs also provide a novel research tool for immature germ cell tumors.

Materials and Methods

Generation of Completely β-catenin-deficient Embryos

To produce oocytes with a single gene deleted, floxed mutant mice on a C57BL/6J background with exon 2–6 flanked by loxP on the β-catenin gene (*Ctnnb1*) [10] were crossed with transgenic (Tg) mice on a C57BL/6J background expressing cre-recombinase in an oocyte-specific manner under the control of oocyte-specific zona pellucida glycoprotein 3 (ZP3) promoter ($Tg^{ZP3-cre}$), which was kindly provided by Dr. Barbara B. Knowles (the Jackson Laboratory, ME, USA). The F1 offspring, β-catenin$^{floxed/floxed}Tg^{ZP3-cre}$ (β-cat$^{fl/\Delta}$), were propagated through brother-sister mating. The presence of the cre-recombinase gene in these offspring was detected by polymerase chain reaction (PCR) analysis using the following set of primers: Cre-S [tgatgaggttcgcaagaacc; nucleotide no. 170 to 189 (GenBank Accession no. AB449974.1)] and Cre-A [ccatgagtgaacgaacctgg; nucleotide no. 539 to 558 (GenBank Accession no. AB449974.1)]. This primer set yielded a band of 389 bp. Furthermore, to produce conditionally β-catenin-deficient sperm, β-catenin$^{floxed/floxed}$ (β-cat$^{fl/fl}$) mice were mated with mice expressing cre-recombinase driven by protamine promoter [11], which was kindly provided by Dr. Masaru Okabe (Osaka University, Japan). We produced β-catenin$^{floxed/floxed}Tg^{protamin-cre}$ male mice, and confirmed that the β-catenin gene was deleted in their epididymal sperm (data not shown). Then, to obtain completely β-catenin-deficient embryos, these two strains of mice were crossed. The β-catenin-deficient (β-cat$^{\Delta/\Delta}$) fertilized eggs were collected and cultured to the blastocyst stage at 37°C and 5% CO_2 in air.

Mouse ESC Establishment and Cell Culture

Embryo-derived stem cells were established using mouse ESCs derivation medium of knockout DMEM (Life Technologies, CA, USA) supplemented with 15% knockout serum replacement, 1 x non-essential amino acids (NEAA), 0.05 mM 2-mercaptoethanol, 2 mM GlutaMax, 100 U/mL penicillin G, 10 mg/mL streptomycin (all from Life Technologies), 1000 U/mL of leukemia inhibitory factor (LIF) (Wako, Japan) and the MEK kinase inhibitor PD98059 (Cell Signaling Technology, Danvers, MA). The blastocyst embryos developed from β-catenin-deficient fertilized eggs were individually treated with EmbryoMax Acidic Tyrode's Solution (Merck Millipore, Germany) to remove the zona pellucidae and plated on a feeder layer. Mouse embryonic fibroblasts (MEF) were inactivated by gamma irradiation in gelatinized culture dishes with mouse ESCs derivation medium. At 48 hours after plating, one half volume of fresh medium was added to each culture well. The medium was changed daily and inner cell mass-derived outgrowths were dislodged with a Pasteur pipette, washed in a drop of fresh mouse ESC derivation medium and incubated for 5 min in StemPro Accutase (Life Technologies) at 37°C. The clumps were gently dissociated with a Pasteur pipette and transferred onto a fresh plate of MEF [12]. β-cat$^{\Delta/\Delta}$ mESCs were maintained in mESC medium which was composed of derivation medium without PD98059. β-cat$^{\Delta/\Delta}$ mESCs were continuously passaged every 2–3 days with 5- to 10-fold dilution by Accutase digestion. For serum-free and feeder-free cultures, mESCs were cultured in N2 and B27 medium (Life Technologies) supplemented with 1,000 U/ml LIF, 3 μM CHIR99021 (Wako) and 1 μM PD0325901 (Wako) on Matrigel-coated (BD Biosciences, San Jose, CA) dishes [13,14]. β-cat$^{fl/fl}$ and β-cat$^{fl/\Delta}$ mESC lines were derived directly either from β-cat$^{fl/fl}$ or β-cat$^{fl/\Delta}$ blastocysts, respectively. The NCH4.3 ESC line (C57BL/6J) [15] and R1 ESC line (129/Sv × 129/Sv-CP) [16] were used as additional controls. The R1 ES cell line was generously provided by Dr. Andras Nagy (Mount Sinai Hospital, Toronto, Canada). F9 embryonal carcinoma (EC) cells were also used as a control in quantitative PCR array experiments. F9 EC cells were grown in a monolayer culture in DMEM (Life Technologies) containing 10% fetal bovine serum (FBS; Hyclone, Thermo Fisher Scientific Inc., UT, USA), 2 mM GlutaMax, 100 U/mL penicillin G and 10 mg/mL streptomycin (all from Life Technologies).

To detect different combinations of fl/fl, fl/Δ and Δ/Δ β-catenin alleles, the genomic PCR was performed using the following primer: (aaggtagagtgatgaaagttgtt, caccatgtcctctgtctattc and tacactattgaatcacagggactt). The resulting products of 221, 324 and 500 bp corresponded to the wild-type allele, the floxed allele and the deleted allele, respectively [9,10].

Differentiation Assays *in vitro* and *in vivo*

For induction of differentiation *in vitro*, 1×10^4 feeder-independent mESCs were plated onto each well of 96-well plate with a low attachment surface (Lipidure; NOF corporation, Japan) and cultured in differentiation medium containing Knockout DMEM (Life technologies) with 20% FBS (Hyclone, Thermo Fisher Scientific), 1×NEAA, 2 mM GlutaMax, 100 U/mL penicillin G and 10 mg/mL streptomycin (all from Life Technologies), to generate embryoid bodies (EBs).

For the tumor formation assay, NCH4.3, β-cat$^{fl/fl}$ (fl/fl#1 and 2), β-cat$^{fl/\Delta}$ (fl/Δ#2 and 3), β-catenin-reintroduced β-cat$^{\Delta/\Delta}$ and β-cat$^{\Delta/\Delta}$ (Δ/Δ#1, 2, 6 and 8) mESCs lines were suspended at 5×10^6 cells/ml in mESC medium, and 200 μl of the cell suspension (1×10^6 cells) were injected subcutaneously into the dorsal flank of nude mice (Clea Japan, Japan) using a 25-G needle. Three to four weeks after injection, tumors were surgically dissected from the mice. Samples were fixed in phosphate-buffered saline (PBS) containing 4% formaldehyde and embedded in paraffin and subjected to histological examination with hematoxylin and eosin (HE) staining. Small samples of the tissue samples were also collected for RNA isolation.

Construction of β-catenin Constitutively Expression Plasmid

The β-catenin expression vector was constructed as follows. The mCherry was amplified by PCR with primer pairs 5′-BstBI-mCherry (ttcgaaatggtgagcaagggcgagga) and mCherry-Bam-3′ (ggatccttacttgtacagctcgtcca) to add BstBI and BamHI sites to the 5′- and 3′-sites of mCherry (Takara Bio, Japan), and cloned into pCR2.1-TOPO vector (Life Technologies), to create TOPO-mCherry. This mCherry fragment was excised from TOPO-mCherry by *Bst*BI and *Bam*HI digestion, and inserted into the

BstBI and BamHI site of pIREShyg3 vector (Takara Bio), to create pCMV-mCherry-hyg. To add the 2A peptide sequence to the 3′-end, mouse β-catenin was amplified by PCR with primer pairs 5′-Nhe-Koz-Catnb (gctagcaccatggctactcaagctgacctgatggagttg) and Catnb-T2A-Cla-3′ (atcgattgggccaggattctcctcgacgtcaccgcatgttagcagacttcctctgccctctccggagcccaggtcagtatcaaaccaggccagc) and cloned into pCR2.1-TOPO vector, to create TOPO-Catnb-2A. This β-catenin-2A fragment was excised from TOPO-Catnb-2A by *Nhe*I and *Cla*I digestion, and inserted into the NheI and BstBI sites of pCMV-mCherry-hyg vector, to create pCMV-Catnb-2A-mCherry-hyg. To generate a piggyBac vector carrying a CAG promoter–driven β-catenin-2A-mCherry, β-catenin-2A-mCherry fragment was first amplified by PCR with primer pairs of 5′-Xho-Koz-Catnb (ctcgagaccatggctactcaagctgacctg) and Catnb-Bam-Cla-3′ (atcgatggatccttacttgtacagctcgtcc), then cloned into pCR2.1-TOPO vector, to create TOPO-Catnb-2A-mCherry. This β-catenin-2A-mCherry fragment was excised from TOPO-Catnb-2A-mCherry by *Xho*I and *Cla*I digestion, and inserted into the XhoI and ClaI sites of the pPB-CAG-EBNXN vector, kindly gifted by Dr. A Bradley (Wellcome Trust Sanger Institute, UK) [17], to create pPB-CAG-Catnb-2A-mCherry. All PCR-amplified fragments were verified by sequencing.

Transfection

β-cat$^{\Delta/\Delta}$ mESCs were washed with PBS once, detached by Accutase and suspended in mESC derivation medium. Cells were dissociated into a single-cell suspension by vigorous pipetting and counted. Pellets of 2×10^6 cells were made and mixed with 1 μg of the β-catenin expression vector and 1 μg of the hyperactive piggyBac transposase expression vector (pCMV-hyPBase), kindly gifted by Dr. A Bradley, in 100 μl of mouse ES cell nucleofector solution (Lonza, Swiss). The cell suspension was transferred to a cuvette and electroporated using an Amaxa Nucleofector device (Lonza) with program A30 following the manufacturer's protocol. The electroporated cells were plated onto 60 mm dishes on MEF in mESC medium. The mCherry-positive colonies were picked up and the clonal lines were maintained as rescued β-cat$^{\Delta/\Delta}$ mESC (res-β-cat$^{\Delta/\Delta}$ mESC).

Karyotypic Analysis

Chromosome karyotyping was carried out at the Nihon Gene Research Laboratories, Miyagi, Japan).

Alkaline Phosphatase Staining and Immunocytochemistry

Alkaline phosphatase (ALP) staining for mouse ESCs was carried out using an alkaline phosphatase kit (Dako, Denmark) according to the manufacturer's protocol. Immunohistochemistry was carried out on mouse ESCs or EBs seeded on gelatin covered 35 mm glass coverslips (IWAKI, Japan) after fixation with 4% paraformaldehyde, followed by permeabilization in PBS with 0.5% Triton-X and blocking with PBS containing 5% normal serum appropriate for each antibody. Incubation with primary antibodies against Oct3/4 (sc-5792; Santa Cruz Biotechnology, Ca), Nanog (rcab0001P; ReproCell, Japan), Sox2 (ab5603; Merck Millipore, Germany), E-cadherin (M108; Takara Bio), β-catenin (C7207; Sigma-Aldrich, MO), α-catenin (C2081; Sigma-Aldrich), Tuj-1 (G7121;Promegam, WI), Desmin (D1033; Sigma-Aldrich), Afp (MAB1368; R&D Systems, MN) and Plakoglobin (610253; BD Biosciences) was carried out overnight at 4°C. Incubation with corresponding secondary anti-mouse, anti-rabbit and anti-goat antibodies coupled with Alexa 488 or Alexa 546 (BD Biosciences) containing 4′,6-diamidino-2-phenylindole (DAPI) for nuclei staining was carried out for one hour at room temperature in the dark in PBS containing 0.1% bovine serum albumin. Staining was observed under a LSM 720 laser scanning confocal microscope.

Tumor samples were fixed in PBS containing 4% formaldehyde and embedded in paraffin. Sections were stained with the following primary antibodies: anti-keratin5/8 (sc-70928; Santa Cruz Biotechnology), Desmin (D1033; Sigma-Aldrich), NeuN (MAB377; Merck Millipore), Oct3/4 (sc-5279; Santa Cruz Biotechnology), pan- Cytokeratin (cytokeratin 5, 6 and 8) (ab6401; abcam, UK), Sall4 (H00057167 1:100; Abnova, Taiwan), β-catenin (C7207; Sigma-Aldrich).

Quantitative RT-PCR Analyses and Genotyping

RNA was isolated using the RNeasy Mini Kit (QIAGEN, Germany). Single strand complementary DNA was synthesized from 1–2 μg of total RNA in 20 μl of reaction mixture containing oligo-dT or random primers using the Superscript III first strand cDNA synthesis system (Life Technologies). We used two types of chemistries for the quantitative reverse transcription polymerase chain reaction (qRT-PCR); TaqMan probe-based [TaqMan Array Mouse Stem Cell Pluripotency Panel (P/N 4385363): Life Technologies] and SYBR Green-based (Platinum SYBR Green qPCR SuperMix-UDG: Life Technologies) systems. Transcript levels were determined using the ABI PRISM Sequence Detection System 7900HT (Life Technologies). All qRT-PCRs using SYBR Green were carried out in triplicate, and relative quantification was carried out using Gapdh as a reference gene. Actb, Gapdh and Eef1a1 were used as endogenous controls when we analyzed gene expression using the TaqMan Array. Hierarchical clustering analyses were performed using Ct values for gene expression data with MEV v4.8 statistical analysis software. The primers used were as follow: Oct3/4, F tgttcccgtcactgctctgg and R ttgccttggctcacagcatc; Nanog, F cctgattcttctaccagtccca and R ggcctgagagaacacagtcc; Lefty1, F gctacaacacagccatgcca and R cctcttttgcctccggagag; Afp, F ccatcacctttacccagtttgt and R cccatcgccagagtttttctt; T, F ctcggattcacatcgtgagag and R aaggctttagcaaatgggttgta; NeuroD1, F acagacgctctgcaaaggttt and R ggactggtaggagtagggatg; Ctnnb1, F ctcaccaccgcgagggcttg and R gcagtccaccagctaggcgc; Tcf3, F gacagaagtggaatttgtgtccg and R agtgcctgctactttctacgat; Sox2, F gcggagtggaaacttttgtcc and R cgggaagcgtgtacttatcctt; Klf4, F aacctttcacactgtcttcccacg and R cccttggactcttccttttctcctg; Axin2, F gcaggagcctcacccttc and R tgccagtttctttggctctt; Sox17, F agccatttcctccgtggtgt and R aacactgcttctggccctcag; Nestin, F tgcatttccttgggataccag and R cttcagaaaggctgtcacaggag; Gapdh, F tgcgacttcaacagcaactc and R cttgctcagtgtccttgctg.

Western Blot Analysis

Western blots were carried out as described by Ishii et al. with slight modification [18]. Western blots were carried out using the following antibodies: β-catenin (C-7738; Sigma-Aldrich), Oct3/4 (sc-5279; Santa Cruz Biotechnology), Nanog (REC-RCAB0002PF; ReproCell) and β-actin (F3777; Sigma-Aldrich).

Blastocyst Injections to Produce Chimeras

To visualize the *in vivo* contribution of β-cat$^{\Delta/\Delta}$ mESCs, β-cat$^{\Delta/\Delta}$ mESCs, were transfected with the constitutive enhanced green fluorescence protein (EGFP) expression vector (pCAG-EGFP) [19]. After screening, we isolated the GFP-positive β-cat$^{\Delta/\Delta}$ mESC (EGFP-β-cat$^{\Delta/\Delta}$ mESC) line, which was continuously cultured on feeder layers in mESC derivation medium with LIF. EGFP-β-cat$^{\Delta/\Delta}$ mESCs were injected into blastocysts of ICR mice, then transferred to the uteri of pseudopregnant ICR mice, as described previously [15,20]. Res-β-cat$^{\Delta/\Delta}$ mESCs with mCherry fluorescence were used for blastocyst injections as donor cells. Embryos

were dissected either on embryonic day (E) 10.5 or 12.5 and the contribution of mESCs to embryos was assessed using a fluorescence stereomicroscope (MVX10, OLYMPUS, Japan).

Animal Studies

All animal experiments were performed according to protocols approved by the Institutional Animal Care and Use Committee of the National Research Institute for Child Health and Development (NRICHD, Permit Number: A2006-009). Mice were housed in plastic cages lined with soft wood chips. The cages were kept in a conventional, air-conditioned mouse room under a 12 h light/dark cycle and the mice received food and water *ad libitum*. All the transgenic mice were monitored for signs of suffering including tumor formation and weakening at least every two days. All surgery was performed under isoflurane anesthesia. Mice were euthanized by carbon dioxide inhalation at humane endpoints or before the collection of embryos and tissue samples as recommended by the American Veterinary Medical Association Panel on Euthanasia. All experiments were subject to the 3 R consideration (refine, reduce and replace) and all efforts were made to minimize animal suffering, and to reduce the number of animals used.

Results

Characterization of β-catenin Deficient Mouse Embryo-derived Stem Cells

We have previously reported the role of β-catenin in sperm-oocyte adhesion using transgenic mice containing oocyte- and sperm-specific cre-recombinase [9]. Using these mouse models, we produced β-catenin-deficient blastocysts by collecting two-cell embryos and developing them *in vitro*. The success rate for achieving blastocyst development was around 80%. We established 12 independent stem cell lines from β-catenin-deficient blastocysts and referred to them as β-cat$^{\Delta/\Delta}$ mESCs (Δ/Δ1–12) (Figure 1A). PCR genotyping of the β-cat$^{\Delta/\Delta}$ mESCs verified the deletion of exon 2–6 of β-catenin (Figure 1B). In addition, western blot analysis confirmed the absence of β-catenin protein in all the β-cat$^{\Delta/\Delta}$ mESCs lines tested (Figure 1C). Furthermore, immunocytochemistry confirmed the absence of β-catenin protein, in contrast to wild-type mESCs, which showed staining of β-catenin in both the nucleus and cell membrane, whereas α-catenin and E-cadherin staining and distribution were similar to β-cat$^{fl/fl}$ mESCs (Figure 1D). Plakoglobin was firmly stained in β-cat$^{\Delta/\Delta}$ mESCs (Figure S7). β-cat$^{\Delta/\Delta}$ mESCs showed similar proliferation behavior and morphological appearance to β-cat$^{fl/fl}$ mESCs. This adaptation of β-cat$^{\Delta/\Delta}$ mESCs is likely due to compensatory upregulation of plakoglobin, which can substitute for β-catenin in cell-adhesion junctions of mESCs [7,8]. The embryos of the loss-of-function mutation of β-catenin developed to the blastocyst stage *in vitro*, but the crossbred female mice produced β-catenin-deficient embryos that died at E7.0 post-conception [9,21,22]. We randomly chose several β-cat$^{\Delta/\Delta}$ mESCs lines for further analysis.

The β-cat$^{\Delta/\Delta}$ mESCs were morphologically similar to β-cat$^{fl/fl}$ mESCs, expressed Alkaline Phosphatase, and were karyotypically normal (Figures 1A, S1A). Pluripotency factors such as Oct3/4 and Nanog were immunocytochemically positive in the nuclei of both β-cat$^{fl/fl}$ and β-cat$^{\Delta/\Delta}$ mESCs (Figure 1E). The expression levels of pluripotent marker genes (Oct3/4, Nanog, Klf4 and Sox2) and proteins (Oct3/4 and Nanog) in β-cat$^{fl/fl}$ and β-cat$^{fl/\Delta}$ mESCs were comparable to those of β-cat$^{\Delta/\Delta}$ mESCs, as assessed by quantitative RT-PCR (qRT-PCR) analysis and western blotting (Figures S1B, S2). Multiple gene expression analysis by qRT-PCR using TaqMan Array Mouse Stem Cell Pluripotency Card showed that β-cat$^{\Delta/\Delta}$ mESCs were similar to wild-type and res-β-cat$^{\Delta/\Delta}$ mESCs (Figure S5A).

To further confirm the functional deficiency of β-catenin in β-cat$^{\Delta/\Delta}$ mESCs in culture, we expanded β-cat$^{\Delta/\Delta}$ mESCs under serum- and feeder-free conditions using the 2i+LIF system with mitogen-activated kinase kinase (MEK) inhibitor, PD0325901, and GSK3β inhibitor, CHIR99021 [13,14]. β-cat$^{\Delta/\Delta}$, under the serum- and feeder-free conditions using the 2i+LIF system, β-cat$^{fl/\Delta}$, and β-cat$^{fl/fl}$ mESCs showed a similar rate of cell proliferation (Figure S1C). We could maintain β-cat$^{\Delta/\Delta}$ mESCs under the 2i+LIF system as β-cat$^{fl/fl}$ mESCs, although partial colonies exhibited a different morphology than previously reported [7] (Figure S3A). We examined Axin2 expression levels in β-cat$^{fl/fl}$ and β-cat$^{\Delta/\Delta}$ mESC (Figure S3B) using qRT-PCR. Exposure to GSK3β inhibitor (2i+LIF) increased the expression of Axin2 in β-cat$^{fl/fl}$ mESCs, while down-regulating Axin2 in β-cat$^{\Delta/\Delta}$ mESCs (Figure S3B). Accordingly, the endogenous Wnt/β-catenin/Tcf/Lef-regulated gene Axin2 was not up-regulated in our β-cat$^{\Delta/\Delta}$ mESCs (Figure S3B). Thus, we further confirmed that β-cat$^{\Delta/\Delta}$ mESCs are defective in the Tcf/Lef-mediated signaling of the canonical Wnt/β-catenin pathway.

Overall, we successfully derived stem cells that were capable of self-renewal directly from β-catenin-deficient preimplantation embryos. These β-cat$^{\Delta/\Delta}$ mESCs can maintain clonogenicity in culture either with or without feeders in serum-free conditions. Thus β-catenin is not required for self-renewal in mESCs.

Differentiation Defects of Embryo-derived β-cat$^{\Delta/\Delta}$ mESCs in EBs and Blastocyst Complementation Assays

We sought to determine whether β-cat$^{\Delta/\Delta}$ mESCs have impaired differentiation potential compared to wild-type mESCs. We created EBs in differentiation medium without LIF from β-cat$^{fl/fl}$, β-cat$^{\Delta/\Delta}$ and β-catenin-reintroduced β-cat$^{\Delta/\Delta}$ mESCs. β-cat$^{\Delta/\Delta}$ EBs were smaller in size compared to β-cat$^{fl/fl}$ EBs (Figure 2A). The extent of the defect in differentiation in β-cat$^{\Delta/\Delta}$ EBs was assessed by immunofluorescence staining for differentiation markers after 14 days. Multiple germ layer formation was severely impaired in β-cat$^{\Delta/\Delta}$ EBs, but not β-cat$^{fl/fl}$ EBs (Figure 2B). At the transcription level, early differentiation markers such as Sox17, and brachyury (T) were detectable on day 6 of EB induction in β-cat$^{fl/fl}$ EBs, but transcripts of these genes were expressed at much lower level in β-cat$^{\Delta/\Delta}$ EBs (Figure 2C). Our results of extremely down-regulated expression of brachyury (T) in β-cat$^{\Delta/\Delta}$ EBs are in agreement with previous findings that brachyury (T) is a direct transcriptional target of β-catenin [23].

To assess the contribution of embryo-derived β-cat$^{\Delta/\Delta}$ mESCs *in vivo*, we performed a chimera assay by blastocyst injection using EGFP-β-cat$^{\Delta/\Delta}$, β-cat$^{fl/fl}$ and β-cat$^{fl/\Delta}$ mESC lines. EGFP-β-cat$^{\Delta/\Delta}$ mESCs were stably maintained with constitutive EGFP expression (Figure 2D). Different lines of EGFP β-cat$^{\Delta/\Delta}$ mESCs were injected into blastocysts and transferred into pseudopregnant mice and the thirty-eight resulting live offspring exhibited no chimeric phenotype. In contrast, the live pups from β-cat$^{fl/\Delta}$ and β-cat$^{fl/fl}$ mESC lines showed high concentrations of the chimeric phenotype (Figure 2F). To further evaluate the ability of β-cat$^{\Delta/\Delta}$ mESCs to differentiate *in vivo*, EGFP-β-cat$^{\Delta/\Delta}$ mESC-injected embryos were recovered on E12.5. Macro zoom fluorescence microscopy images revealed that the contribution of EGFP-β-cat$^{\Delta/\Delta}$ mESCs was barely detectable in whole body embryos on E12.5 (Figure 2E), although a small contribution was rarely detected in some malformed fetuses (Figure S6). Taken together, embryo-derived β-cat$^{\Delta/\Delta}$ mESCs are significantly impaired in their ability to differentiate properly *in vitro* and *in vivo*.